POLITECNICO
MILANO 1863

SCUOLA DI INGEGNERIA INDUSTRIALE
E DELL'INFORMAZIONE

Adding time dependence to the Resident Space Object Network

Tesi di Laurea Magistrale in
Space Engineering - Ingegneria Spaziale

Author: **Davide Contaldo**

Student ID: 993622
Advisor: Prof. Camilla Colombo
Co-advisors: Prof. Jérôme Daquin, Dr. Matteo Romano
Academic Year: 2023-2024

Abstract

Space, especially in Low Earth Orbits (LEOs), got progressively more clogged as the years went by, and the trend does not seem to change. This incessant growth in the number of Resident Space Object (RSO)s has generated concern in the space community, that started to face the problem. In order to study the conditions in which the space environment is and the related risks of collision of the RSO in near-Earth orbits, several models have been designed. The majority of them offer an individual view on the matter, analysing the risks object per object. A few of them, based on network theory, have been designed in order to have a more cohesive view on the space debris problem, allowing to consider each RSO and each probability of collision as a component of a larger system. The model taken as starting point for this work is the Resident Space Object Network (RSONet) designed by Romano et al. [1], [2]. This method exploits graphs and their properties in order to analyse the probability of collision of the various RSO over a simulated time period. This is done by defining a score S, that evaluates the overall probability of collision of each RSO with the others, summing different contributions each representing a different way two RSOs can interact, directly or indirectly. This score allows to properly weight how each RSO contributes to the collision risk within the population and identify the most relevant objects. The object of this work is to expand the RSONet by introducing time dependence, by making possible collisions at a given time conditional on the previous events that might have involved each RSO. This addition allows to obtain a greater realism within the model and a new definition of a score that estimates the overall risk of collisions more accurately. The process followed to apply the several modifications, the new contributions derived for the time-varying scenario and some interesting results comparisons are presented. The new time-framed model is applied to the RSONet and compared to the static model to discuss the differences and advantages, regarding the networks and the scores. Applications to study space environment and to methods for Active Debris Removal (ADR) and Collision Avoidance Manoeuvres (CAM) are suggested, that could make use of the peculiarities of this model.

Keywords: networks; RSONet; time dependence; collision probability; space environment; active debris removal; collision avoidance manoeuvres

Abstract in lingua italiana

Lo spazio, specialmente nelle LEOs, è diventato progressivamente più congestionato col passare degli anni, e la tendenza non sembra cambiare. Questa crescita incessante nel numero di RSOs ha generato preoccupazione nella comunità spaziale, che ha iniziato ad affrontare il problema. Per studiare le condizioni in cui si trova l'ambiente spaziale e i rischi di collisione relativi ai RSOs nelle orbite vicine alla Terra, sono stati progettati diversi modelli. La maggior parte di questi offre una visione individuale della questione, analizzando i rischi oggetto per oggetto. Alcuni di essi, basati sulla teoria delle reti, sono stati progettati per offrire una visione più coesa del problema dei detriti spaziali, permettendo di considerare ogni RSO e ogni probabilità di collisione come componente di un sistema più grande. Il modello preso come punto di partenza per questo lavoro è il RSONet progettato da Romano et al. [1], [2]. Questo metodo sfrutta i grafi e le loro proprietà per analizzare la probabilità di collisione dei vari RSOs nel periodo di tempo simulato. Questo viene fatto definendo un punteggio S, che valuta la probabilità complessiva di collisione di ciascun RSO con gli altri, sommando diversi contributi, ciascuno rappresentante un diverso modo in cui due RSO possono interagire. Questo punteggio permette di analizzare correttamente come ogni RSO contribuisce al rischio di collisione all'interno della popolazione e identificare gli oggetti più rilevanti. L'obiettivo di questo lavoro è espandere il RSONet introducendo la dipendenza temporale, rendendo le possibili collisioni in un dato intervallo dipendenti dagli eventi precedenti che potrebbero aver coinvolto ciascun RSO. Questa aggiunta permette di ottenere un maggiore realismo all'interno del modello e una nuova definizione di punteggio che stima il rischio complessivo di collisioni in modo più accurato. Viene presentato il processo seguito per applicare le diverse modifiche, i nuovi contributi derivati dalla dipendenza temporale e alcuni interessanti confronti di risultati. Il nuovo modello temporale viene applicato al RSONet e confrontato con il modello statico per discutere le differenze e i vantaggi. Vengono quindi proposte applicazioni allo studio dell'ambiente spaziale, oltre a metodi per ADR e CAM, che potrebbero sfruttare le peculiarità di questo modello.

Parole chiave: reti; RSONet; dipendenza temporale; probabilità di collisione; ambiente spaziale; rimozione attiva di detriti; manovre anti-collisione

Contents

1 | Introduction

On January 11, 2007, the Chinese military destroyed the weather satellite Fengyun-1C, causing a space debris generating event that has contributed greatly to the growth in the number of space debris in LEOs [3]. Two years later, on February 10, 2009, Iridium 33, an active communications satellite, collided with Cosmos 2251, an inactive military communications satellite. This was the first occurrence of an active satellite being destroyed in a collision with a debris. These two events increased the number of debris in LEOs by the 50% [3].

In addition to these collision events, the other factor contributing to the overcrowding of the space environment is the rate of spacecraft being launched, a trend that is constantly increasing [4]. The growth in the number of active spacecrafts deployed in LEOs contributes greatly to the progressively bigger problem of overcrowding and, consequently, to the space debris problem.

This brief analysis highlights the importance of studying the space environment in order to reduce the possibility of collisions. Since the late 70s, the possible effects of overcrowding have been studied. The formulation of the so called *Kessler Syndrome* effect can be traced back to 1978, as proposed by Donald j. Kessler, a National Aeronautics and Space Administration (NASA) scientist [5]. According to his predictions, the continuous growth in number of orbiting objects in LEOs would eventually create a scenario where fragmentation cascading effects would be much frequent, with these effects being visible starting from the 21^{st} century. This would lead to a congested environment in which space missions and new launches could be threatened by the higher risk of collisions, passing through or being inserted into this crowded belt [5]. While it is still unclear if this scenario is already in place or not, there is a clear need of solutions that could contribute cleaning up the space environment, especially in LEOs [6].

The space industry has been experiencing a constant growth since its birth, and new contenders are emerging alongside historical competitors in the last 15-20 years. Both private companies, such as SpaceX, with its Starlink mega-constellation, or Blue Origin, both born in the first years of the 2000s, and public entities, such as Vietnam and Bolivia, have new space programs and strive to access space [7]. As a consequence, the number of

launches is constantly rising, as shown in Fig. 1.1, and so is the number of payloads in orbit [8].

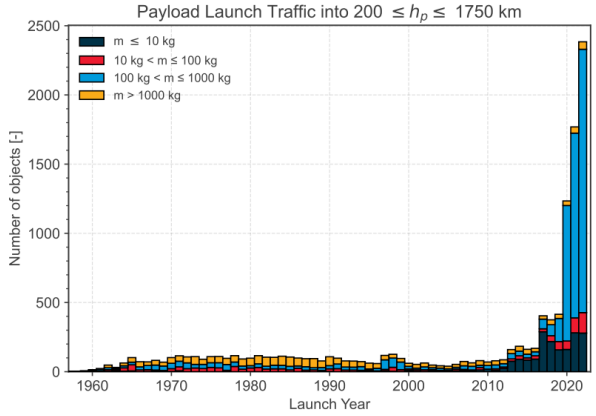

Figure 1.1: Payload launch traffic into $200 \leq h_p \leq 1750$ km, from [9].

At the same time, space debris in LEOs orbits are increasing, and this influences both ongoing missions and new launches. Over the last 20 years almost 12 fragmentation happened per year on average [10], and their trend is visible in Fig. 1.2. Data show a

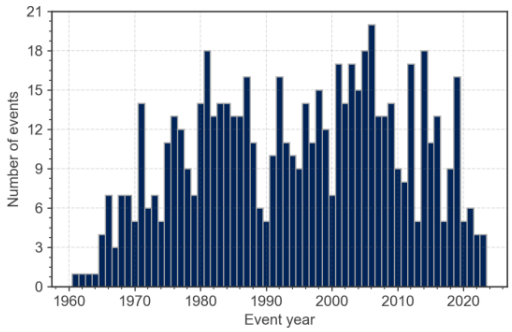

Figure 1.2: Number of fragmentation events per year, from [11].

currently growing pattern and the number is bound to inflate. Projections show that the presence of space debris will increase if action is not taken, even if no new launches were to be carried out. This is due to the cascade effect that would be caused by each collision between already orbiting objects, generating new debris on impact [12]. According to European Space Agency (ESA), the number of events, consisting in explosions, break-ups and collisions, that then resulted in a fragmentation is more than 640 [13]. These accidents have participated in increasing the number of space debris of various size. Even though an already high number of them, consisting in more than 36000, is constantly monitored, it is estimated that there are more than 130 millions under 1 cm of size [13].

Different studies have been carried out to address the rising problem of space debris along the years. ESA took the initiative with the Zero Debris policy, a document suggested by Member States in Autumn 2022. The purpose of this approach is to reduce debris production in Earth and Lunar orbits [14]. Various recommendations have been thought of regarding different aspects of a space mission, with the accent posed on disposal, collision avoidance, health monitoring to avoid explosions and intentional debris release. Following these guidelines would ideally allow to invert the tendency of European contribution to space debris growth.

Some steps have been taken in the direction of reducing the number of already existing debris. Active debris removal missions are of fundamental importance for cleaning space. ClearSpace-1 is the first mission with the purpose of removing a derelict object from orbit, designed and developed by Swiss start-up ClearSpace SA and ESA [15]. The other main step which research and efforts should work towards is implementing and improving methods to avoid creating new debris. In line with this purpose, a few models to give an estimate on the space debris situation have been developed. The scope is to use these models in order to increase awareness of space condition and give instruments to better design the space segment to companies and agencies that want to access space. Having information about close encounters that a spacecraft might experience, either with other operating spacecraft or with debris, is fundamental in order to perform collision avoidance manoeuvres. Moreover, having a general knowledge of space debris relative dynamics, or their connections in terms of Minimum Orbital Intersection Distance (MOID), would provide necessary information on how to choose the best candidates for active debris removal [16].

Raising awareness on the space debris topic is then a further step, needed in order to start confronting the problem at mission design level [17]. This would hopefully lead to progressively more "space environment friendly" missions, that plan for shorter end-of-life, thus decreasing the probability of collision with other orbiting objects. Related to this topic, some new guidelines have been thought about along the last years, with ESA trying to provide new approaches to the problem. The already cited Zero Debris policy is the result of such philosophy change. An important recommendation of ESA new approach states the need to comply with a 5 years End-of-Life (EOL), instead of the 25 years previously allowed. This change would lower the probability of collision after the end of operations for a spacecraft by simply reducing its time in orbit. Ideally, the adoption of these guidelines by all members of the Inter-Agency Space Debris Coordination Committee (IADC) would help reduce the growth rate of space debris [14]. This being said, the current guidelines stated by IADC still tend to the "25-year rule", stating that a RSO is naturally compliant if it operates in an orbit such that it does not need manoeuvres in

order to re-enter in less than 25 years [11].
A change in space missions design philosophy, that could also lead to economical benefits, according to NASA analysis [18], would eventually contribute to diminish the probability of creation of new debris, allowing active removal missions to effectively lower the total number of debris. An example of this kind of research is the study carried out by Lawrence et al. [19] analysed the problem by comparing the space environment to an ecosystem. Between the legal and political topics, the importance of protecting the space environment becomes clear in order to persist in the space industry.

1.1. Main sources of debris

The number of space debris in orbit is constantly increasing, for many different reasons. The evolution of RSOs can be seen in Fig. 1.3.

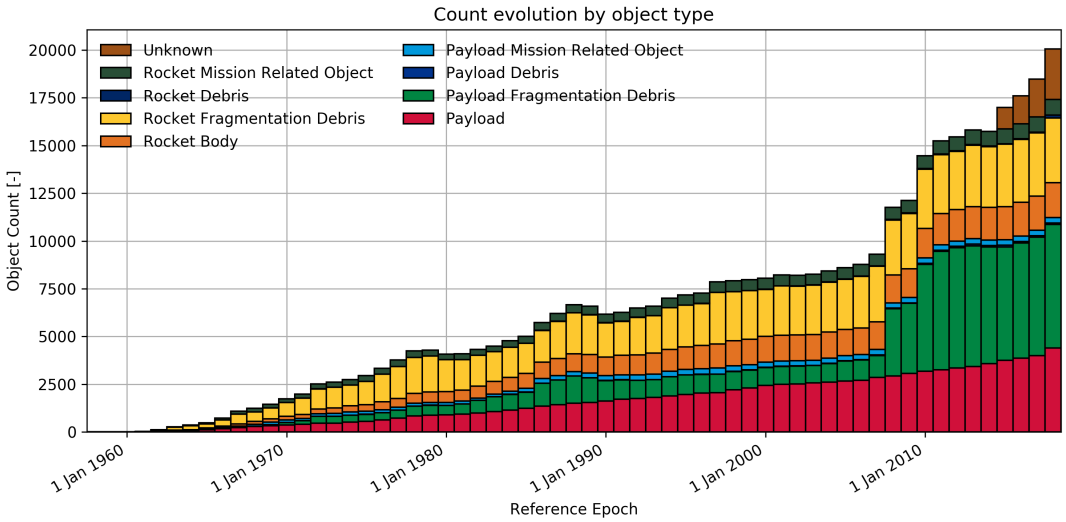

Figure 1.3: Evolution of RSOs over time, from [20].

It is interesting to look at how the trend could be in the following years. In Fig. 1.4 the simulated scenario highlights the growth in number of RSO in LEOs that is probably going to happen in the next 200 years. It is possible to notice how, even in case of no further launches, the number of RSO would increase, due to the collisions of objects already in LEOs. Clearly the curve would be steeper in the realistic case of new launches happening in the following years.
The main fragmentation sources of debris are listed followingly:

- The number of satellites in orbit is constantly increasing, especially due to the

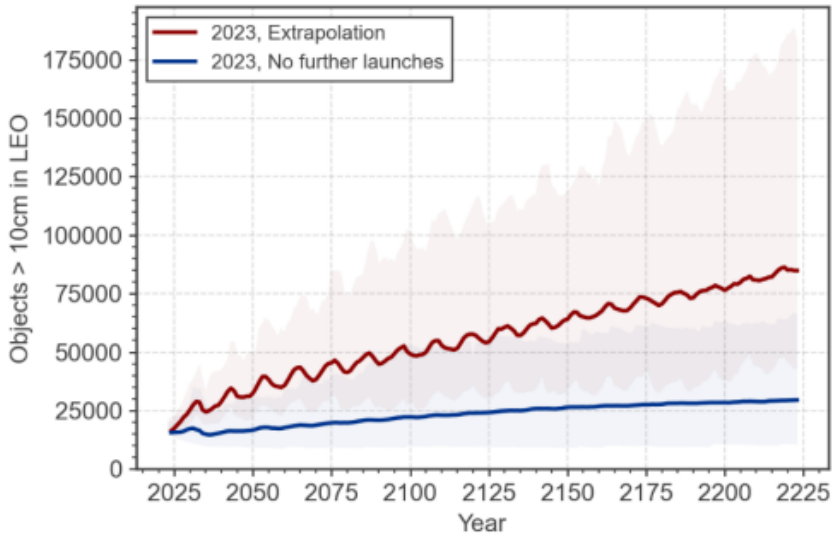

Figure 1.4: Simulation of the number of RSO in LEOs in the following 200 years, from [11].

number of mega-constellations that have been designed and launched in the last few years [21]. The companies responsible for creating a major impact on the number of mega-constellations in orbit are SpaceX, OneWeb, Amazon, Telesat, Iridium Next, Globalstar and Flock [22].

- Collisions and fragmentation are a factor that becomes exponentially more dangerous as the number of RSO grows, possibly causing a cascade effect that can quickly overcrowd the belt in LEOs. This effect is known the aforementioned Kessler Syndrome 1.
- Anti-Satellite (ASAT) tests are a deliberate source of debris. Satellites are destroyed during these tests, generating debris clouds. A recent example of such occurrence is the destruction carried out by the Russian Ministry of Defense of a Russian satellite, causing a debris cloud that could have been dangerous even for the International Space Station (ISS) [23]. Other instances of such tests have been documented and carried out by other spacefaring nations, such as USA [24], India [25] and China, with the already cited destruction of the Fengyun-1C in 2007 [26].
- Explosions of RSOs contributes to increasing the number of orbiting objects. These events are mainly caused by residual energy sources remaining on board of defunct RSO orbiting in LEOs, such as fuel or batteries [20].

Non-fragmentation sources have contributed too, even if less than fragmentation sources, to the increase of debris number in orbit. Between them, some have impacted more than

others on the space population:

- Solid rocket-motor firings introduce a number of small debris in space, especially slug and dust particles. These debris are in the order of millimeters in size and their trajectory passes through the lower parts of the atmosphere, meaning they do not have lingering effects in orbit. Nonetheless, they have an impact on space population for the time needed for them to re-enter atmosphere [27].
- Abandoned spacecrafts and launcher stages constitute a main risk for the still active RSOs in orbit. In the long run, these bodies contribute to the cascade effect that might worsen the conditions of space environment. For this reason, ESA created the aforementioned Zero Debris policy, shifting also the time needed for re-entry from 25 to 5 years after the end of operational life of a spacecraft, as mentioned in Chapter 1 [14].
- Other single events have contributed to the growth of space debris problem. Some examples are droplets of reactor coolant liquid released during the end-of-life of Russian satellites for ocean surveillance during the 80s, or the copper wires release during an experiment carried out in the 60s during Misas missions [20].

This being said, there are other topics to be considered when addressing the space debris problem, mainly the reasons that brought the space environment to the current situation. The main ones that had an impact in the past or are still affecting the current scenario can be highlighted:

- Although there are guidelines that can be followed by any space fairing country and entity, the lack of clear regulations makes it so that none of these guidelines can be enforced. A direct effect is that launching entities tend to avoid addressing the space debris problem, since measures for debris mitigation taken at mission design level are often quite costly.
- Complexity of debris removal technologies affects the efficiency of such methods to keep the growth of fragments in orbit under control.

1.2. Aim of the research

The impact of the space debris problem on the whole space field has been thoroughly explained. Many different ways to study and analyse the space environment have been designed over the years, with different methods created in order to find better models in terms of computational cost, time and accuracy of the results. These methods are going

to be explained in more details in the Chapter 2.1.
The one this thesis mostly focuses on is the one described by Romano et al. [1] [2]. This model focuses on the creation of a score, through the use of network theory, that can reflect the probability of collision that the various RSO have. This approach, that takes the possible conjunctions into account, embedding them in a network, allows to analyse and compare the contribution that each RSO brings to the total risk of collision in LEOs. This means that a more cohesive view on the space environment health can be obtained [1] [2]. This is the main novelty of the approach, that does not focus on the single conjunction events and collision probabilities, like the other models do. The RSO are not seen as individual entities, each with their own probability of collision, analysed independently from the others, but as components of a wider system, in which every object contributes to possibly increase the risk of collisions in orbit. Further details regarding the base model for this research are going to be provided in Chapter 4.
The aim of the thesis is to work on this existing model, improving its fidelity and the accuracy of the probability evaluation when considering the same simulation time. To do so, we add time dependence to the model. In fact, the RSONet considers all close approaches present in the network as if they happen at the same time. By adding time dependence, the purpose is to retrieve more accurate results by modifying the equations used in the previous model accordingly, taking into account the time dependence of the conjunction events. This improvement of RSONet is based on dividing the whole simulation time in time windows for the evaluation of the probabilities of collision. In this scenario, the time step at which a certain event has occurred further influences how the next time step is evaluated. The whole concept is explained in Chapter 5.

2 | State of the art

Addressing the problem of space debris can often be connected to studying statistics and probabilities related to the space environment. However, this approach needs some bases to work. First, space debris need to be identified and tracked. At the beginning of the space era, the United States Air Force created Project Space Track, the first system capable of tracking artificial objects in space. Other systems were later developed, with the same purpose, such as North American Aerospace Defense Command (NORAD) Space Object Catalogue [28]. They use Two-Line Elements (TLEs) [29] to tie orbital parameters, derived from observations in a specific time interval, and other useful information to a specific object in the catalogue.

As the space debris problem became progressively more relevant, different methods have been developed to counteract this growing issue.

Efforts have been made in the past few years in order to study important break-up cases, like the Iridium-Cosmos collision. These analyses of past collisions help the space community to better understand the impact of a similar occurrence on the space population. Pardini, Anselmo [30] studied the case thoroughly, by using the Space Debris Impact Risk Analysis Tool (SDIRAT) to analyse the flux of catalogued objects resulting from the break-up. This method helps evaluating other variables other than the flux, such as relative velocity, impact velocity, debris mass. These values are then studied in order to assess the risk of collision on specific targets [31]. Other tools developed to study and predict the space debris problem are going to be addressed later 2.1.

Tracking the evolution of debris clouds generated from previous impacts is also fundamental in order to constantly improve the break-up models, such as NASA Break-Up Model (BUM) EVOLVE, that has been progressively improved by studying fragmentation in LEOs [32]. Debris clouds are indeed a major aspect in contributing to a faster growth in term of number of space debris in LEOs. From a single collision, hundreds or even thousands of fragments could generate, possibly starting chain reactions, thus making their study a need in order to improve space sustainability.

It is possible to prevent in-orbit break-ups through collision avoidance manoeuvres, that are backed up by a precise tracking of the RSO population. This being said, many re-

searches are focused on the risk that debris pose to the space environment. Various methodologies have been studied, with a fairly common ground for some of them being the formulation of indices, computed in different ways, to have a faster method to assess probabilities of collision, severity of break-ups, risk posed onto the space environment [33]. Some of these methods could also used to provide a thoughtful way of discerning which orbiting objects would most suitable for an active removal mission. Some examples are provided followingly.
Kebschull, Radtke, Krag [34] developed the Environmental Criticality (EC) is a criteria that groups together two useful pieces of information, the risk of fragmentation and its impact on the space environment. A similar approach has been taken in developing the Criticality of Spacecraft Index (CSI). It is an analytic index created by Rossi, Valsecchi, Alessi [35] that considers physical characteristics, the orbit and the environment in which an object is located.
Another analytic index has been later implemented, assessing the effects of a catastrophic fragmentation on the space environment. The study carried out by Letizia et al. [36] utilised the density of the debris cloud to analyse the propagation of the fragments. In this way it is possible to analyse and better understand the impact of fragments clouds on the rest of the orbiting population. This study was the natural evolution of the previous research of Letizia, Colombo, Lewis [37], where the impact of small debris has been thoroughly analysed through their density in LEOs. More precisely, density is exploited to study the evolution of fragments smaller than 10 cm, subjected to the effect of atmospheric drag.

2.1. Models for space debris dynamics analysis

A few methods have already been addressed to in previous sections, such as SDIRAT and EVOLVE. These are just two of the numerous tools developed by various agencies in order to predict the evolution of the space debris environment.
The models that are presented in this and in the following Chapter 2.2 can have many scopes, from highlighting and selecting the most dangerous debris, to assessing the probabilities of collision of RSO. Then they need to be applied to practical actions of various kinds in order to effectively contribute to Space Traffic Management (STM) and the improvement of space environment health. These actions can vary, from CAM [38] to ADR, which are still an important challenge but may lead to great results in terms of cleaning space [39]. These methods are not the focus of this research, but they are going to be addressed in Chapter 7.2, since they are possible applications of the model that is presented

throughout this thesis.
Evolutionary models are designed to study and predict the evolution of the space traffic, useful for studies that aim to analyse the risk related to possible collisions. They can be exploited for long-term projections of space environment, such as Long Term Utility for Collision Analysis (LUCA) [40]. This method uses Monte-Carlo simulations, varying the inputs of initial population, solar activity and other parameters, in order to analyse various plugins, i.e. interesting variables that can be studied in a long-term simulation. These plugins include launch traffic, collision rate determination and also solar and geomagnetic forecasts.
Other models are useful for prediction purposes. Meteoroid And Space debris Terrestrial Environment Reference (MASTER) [41] is a tool developed by ESA to help mission design and risk assessment analyses. It evaluates space debris flux and it can project it to get simulations of it for a few years in the future.
Debris Risk Assessment and Mitigation Analysis (DRAMA) is another one, developed by a team under contract with ESA. This tool, composed of five different software applications, each one addressing a particular aspect of debris mitigation [42]. The provided tools are Assessment of Risk Event Statistics (ARES), MASTER (-based) Impact Flux and Damage Assessment Software (MIDAS), Orbital Spacecraft Active Removal (OSCAR), Spacecraft Entry Survival Analysis Module (SESAM) and Spacecraft Entry Risk Analysis Module (SERAM). They have been designed respectively for assessment of CAM, collision flux, EOL, re-entry and risk posed by re-entering objects surviving the atmosphere. A further explanation can be obtained in the paper written by Martin et al. [42].
Another ESA tool is Debris Environment Long-Term Analysis (DELTA), developed in order to accomplish the goal of studying long term evolution of debris environment. This instrument was ESA answer to the need of better understanding the space environment. It can analyse and simulate space traffic with long-term predictions, useful for many purposes, mainly end-of-life planning. It uses a three-dimensional deterministic model and can evaluate mission collision risks by studying the evolution of a user defined space population over a chosen time span. This model can be used for studying LEOs, Medium Earth Orbits (MEOs) or Geosynchronous Equatorial Orbits (GEOs) [43]. Other agencies created their own models, to assess the situation of space environment up to High Earth Orbits (HEOs).
Many other methods were developed in the 1990s.
Debris Assessment Mitigation Analysis and Growth Evaluation (DAMAGE) analyses long-term evolution of the space environment, while at the same time assessing the effectiveness of debris mitigation measures and spacecraft disposal strategies. It focuses on GEOs and HEOs, and it helps evaluating risks related to spacecrafts operating in those

regions [44].
Integrated Model for the Probabilistic Assessment of Collision Threats (IMPACT) is a hypervelocity collision and explosion model, useful to predict the development of debris clouds generated by any kind of fragmentation events, from collisions to explosions. It uses semi-empirical model to evaluate risk of collision, combining empirical distributions obtained from with analytical techniques [45].
LEO-to-GEO Environment Debris (LEGEND) is a three-dimensional model that can perform simulations of historical and future space debris traffic. It uses two different approaches for its two purposes. While it exploits deterministic approach to study the historical population, it uses Monte-Carlo simulations for studying future breakups and analysing probabilities of collision [46].
Then, NASA developed two methods, Orbital Debris Engineering Model (ORDEM) and Model for Energy Dissipation and Debris Environment Evaluation (MEDEE). The first one is mainly used for analysing current debris population, using data from ground and space segments to build statistical models. An environment model can be built, that describes spatial density of debris in LEOs [47]. MEDEE, on the other hand, is mainly used for assessing energy dissipation due to collisions, evaluating collision probabilities and taking snapshots of the space environment. It is built in modules, each of them in charge of a specific part of the model, from orbit projections to evaluation of collision probabilities. This means that it is easily modifiable without needing to change its whole structure [48].
All these methods can help in better understanding the conditions of space environment, but some practical actions need to be performed in order to make use of these models. The possible applications of these models, that are part of the methods to clean the space of debris,

2.2. Network approach

Among all the different approaches to the space debris problem, the one that is going to be exploited in this work is the network approach.
Some studies have been conducted on the topic. Lewis et al. [49] used networks to describe relationships between Earth satellites, with vertices that represent satellites and debris, while the edges are the possible conjunction events. By doing this kind of analysis, it is possible to identify the RSO that threaten the rest of the space population [49].
Other models exploiting networks have been proposed in the recent years. Some of them exploit temporal networks, like Acciarini, Vasile [50]. They built a multi-layer network that analyses the connections between different RSO, through links and nodes, with each

layer of the network addressing a different type of interaction. These multi-layered models can be used to describe failures and patterns in the space population in a reliable way [51].
Later, a model exploiting the most recent researches on Graph Neural Network (GNN) and machine learning have been designed by Stevenson, Rodriguez-Fernandez, Urrutxua [52]. This model aims to predict the creation of possible conjunctions. The predicted ones are then collected in a graph through the use of GNN, and the three-filter sequence proposed by Casanova, Tardioli, Lemaître [53].
A different methodology has been considered by Romano, Carletti, Daquin [2]. In their research, the attention is focused on obtaining a unified approach to STM through the use of network theory. Thus, a cohesive risk index can be obtained, allowing for a more thorough approach to mission design, that can account for collision risk along the trajectory of the launcher and the orbit of the spacecrafts.
This approach revolves around evaluating a relevance score S, that is defined as the sum of three contributions C_1, C_2 and C_3. Each of these contributions addresses a specific collision scenario.
C_1 evaluates the probability of direct collision between RSO. This is usually the main component of the score for a node, due to how it is evaluated. The degree centrality is fundamental in order to identify its value.
The second contribution C_2 considers the possibility of a collision between a node i and fragments generated by a collision between neighbours of i. In this case, of the clustering coefficient is useful in determining how these more complex interactions may evolve. This contribution grows as the links between nodes increase, and it is used for taking the debris clouds into account in the RSONet environment.
C_3 is the contribution that takes into account possible chain reactions, considering collisions with distant nodes in the topology of the network. This contribution is bound to be smaller than the other two, since it is related to the probability of a sequence of collisions.

3 | Theoretical framework

3.1. Network theory

A brief introduction to network theory is here presented, in order to better understand some concepts that have been used throughout this thesis.
Network theory is a field of study, part of mathematics and computer science, that studies networks and their characteristics, including their structure, behaviour and dynamics. Networks are composed by interconnected nodes (or vertices) and edges (or links).
A few terms that are going to be used in this work need to be defined and explained in the context related to this topic (see Appendix A).
An important mean, used in the thesis, to study the networks is its graph. It is composed by a series of nodes, with edges connecting them. Graphs can be used to study many concepts, other than pure mathematical ones, ranging from sociology to biology and computer science. The nodes may represent individuals, objects, places or even organisations, depending on the field of application, while the edges connect the nodes to each other, acting as the interactions between them.
There are a few different types of networks, granting the possibility of being adaptable to different scenarios and applications:

- Static networks are generated all at once, as if all the connections present in them were to happen at the same time [54].
- Temporal networks are systems that are modeled in order to explicitly have the information about the time at which any interaction in the graph happens [54].
- Undirected networks are composed of edges that connect nodes between each other without any particular order or direction [55]. It is thus possible to move between nodes back and forth.
- Directed networks have the peculiarity of being constituted of edges that can be crossed only towards a specific direction. This means that if a node a is connected to a node b, in general, it is possible that the node b is not connected to the node

a [56].

- Unweighted networks do not have weights related to their edges, meaning that each edge has the same importance and characteristics of the others [57].
- Weighted networks have edges associated to weights, values that identify the strength of the connection between two nodes [58].
- Connected networks are those where any two nodes are connected by a path. These networks can then be strongly connected, if any couple of nodes is connected by a directed path [56].
- Disconnected networks are graphs split in components, that are smaller parts of the graph, themselves composed of nodes and edges [56].

In the proposed work, each node represents an orbiting object, while each edge represents a close approach between orbiting objects.
A fundamental tool is the adjacency matrix A. It is a symmetric square matrix that represents a graph and all the conjunctions that are present in the graph. If the value of the element of the adjacency matrix that relates two nodes is null, then the two nodes are not connected by an edge in the graph identified by said adjacency matrix. On the contrary, when the element of the matrix related to the nodes is not null, the vertices are in fact connected in the graph. This matrix proves to be essential in the research here presented, and its role is going to be explained in detail in Chapter 4.2.

3.2. Probability theory

A short summary of some concepts of probability theory is here presented, since their application is fundamental in order to understand the thesis topics.
Probability theory is fundamental in order to study risk related topics, independently from the application field. The concept of dependence, independence and mutual dependence are followingly described. Let us consider two events A and B, and evaluate the probability of them happening in the three cases.

- Dependent events are those that can be affected by previous events and results. The probability of the two events happening, considering B dependent on A, can be evaluated as $P(A \cap B) = P(A)P(B|A)$, where $P(B|A)$ represents the probability of B happening given that A has happened.
- Independent events are not influenced by any other events. This means that the probability of the two events happening is calculated as $P(A \cap B) = P(A)P(B)$.

- Mutually exclusive events are groups of events where each occurrence can happen only if none of the other ones has happened before. The probability of one of the two events happening can be evaluated as $P(A \cup B) = P(A) + P(B)$.

4 | The Resident Space Object Network

The RSONet has been developed by Romano et al. [1, 2] with the intent of creating a tool for STM tasks. The aim of the research was to shift the focus from the single orbiting objects to the whole space resident population. This would allow for a wider and more general insight on the space environment status. The first formulation of the RSONet also defined a risk score based on the topology of the network and the characteristics of the RSOs, with the goal of estimating the overall risk of collisions among the population and identifying the members which contribute the most to this risk, in order to take actions upon them (e.g. ADR missions).
The score was initially defined by introducing some simplifying hypotheses, in order to reduce the complexity of the problem and allow a fast evaluation of the risk indexes without the need of simulating each possible fragmentation or additional simulations of the RSOs. The key assumptions are the following:

- All the conjunctions of an object i are assumed to be mutually exclusive and independent from time, meaning all close approaches are considered as if happening simultaneously (thus resulting in a time invariant network);
- A distinction between "small" and "large" objects is made, in order to differentiate their behaviour in case of a collision: all objects classified as debris are considered "small" and that cannot create other fragments in case of a collision; on the other hand, every other object in the adopted catalogues is considered "large" enough to generate a debris cloud when colliding, thus possibly starting cascade effects. A binary factor ψ has been introduced in the formulation, with $\psi = 0$ for "small" objects, and $\psi = 1$ for "large" objects.

The RSONet score S as defined by Romano et al. is a risk metric defined individually for each RSO as the sum of three contributions. Each represents a different way two RSOs can interact, either with a direct collision or with an indirect one through the production of fragments which cause new collisions: the first contribution evaluates the probability of

collision of an object i with its neighbours j; The second contribution considers possible collisions between the RSO i and fragments derived from a fragmentation of j; finally, the third contribution evaluates the probability of a chain effect happening by considering collisions with distant RSO in the topology of the network. Thus, using the RSONet as a guide, a risk metric $\mathcal{S}^{(i)}$ for each object i in the network is defined, which combines the three contributions $\mathcal{C}_1^{(i)}$, $\mathcal{C}_2^{(i)}$, and $\mathcal{C}_3^{(i)}$, respectively. The topology $\mathcal{N}$ of the RSONet translates into the three contributions, as given in Eq. 4.1:

$$\begin{aligned}\mathcal{S}^{(i)} &= \mathcal{S}^{(i)}(\mathcal{N}, p_{ij}, \psi_i, m_i) \\ &= \mathcal{C}_1^{(i)}(\mathcal{N}, p_{ij}, \psi_i) + \mathcal{C}_2^{(i)}(\mathcal{N}, p_{ij}, \psi_i, m_i) + \mathcal{C}_3^{(i)}(\mathcal{N}, p_{ij}, \psi_i, m_i),\end{aligned} \tag{4.1}$$

where p_{ij} is the probability of collision between objects i and j during a conjunction, ψ_i is the binary coefficient representing the type of object ("large" with $\psi_i = 1$, or "small" with $\psi_i = 0$), and m_i is the mass of the RSO which is used to estimate the number of fragments produced during a fragmentation (thus used only in the second contribution), via the NASA break-up model [32]. This score allows to properly weight how each RSO contributes to the collision risk within the population.

The first contribution $\mathcal{C}_1$ takes into consideration the possible collision of an object i with its j neighbours, and is defined as follows (Eq. 4.2):

$$\mathcal{C}_1^{(i)} = \sum_j (\psi_i + \psi_j) p_{ij}, \tag{4.2}$$

where p_{ij} represents the probability of a collision between i and j during a conjunction, which becomes relevant only if at least one object is classified as "large", while goes to zero if it involves "small" objects. The rationale behind the first contribution can be seen more clearly in Fig. 4.1.

The second contribution $\mathcal{C}_2$ considers the possibility of a collision between an object i and fragments generated by a collision between neighbours of i, as shown in Eq. 4.3:

$$\mathcal{C}_2^{(i)} = \psi_i \sum_j \psi_j 10^M p_{ij} \hat{p}_j, \tag{4.3}$$

with the factor 10^M used to introduce the size of the debris cloud in calculations. M is, in fact, a term related to the mass of the two orbiting objects involved in the generation of the debris cloud. Then, $\hat{p}_j$ represents the overall probability of a fragmentation of j by a collision or an explosion (even if this latter case is not treated in this work), which can only happen if j is classified as "large". A representation of the idea behind the second

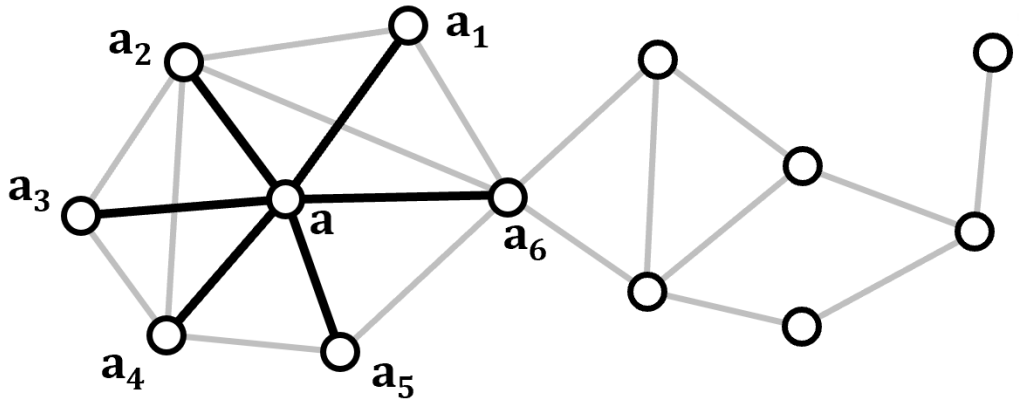

Figure 4.1: Visual representation of the first contribution, from [1].

contribution can be seen more clearly in Fig. 4.2.

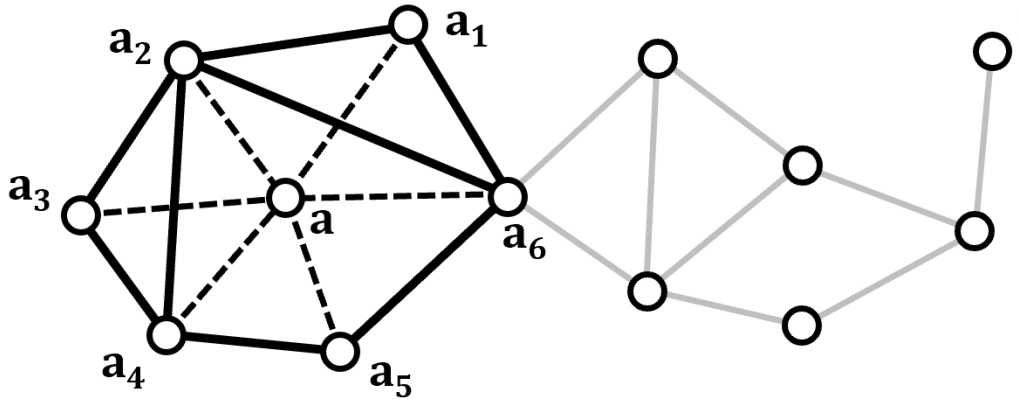

Figure 4.2: Visual representation of the second contribution, from [1].

Finally, the third contribution $\mathcal{C}_3$ takes into account possible chain reactions, considering collisions with distant RSOs in the topology of the network, defined as in Eq. 4.4:

$$\mathcal{C}_3^{(i)} = \psi_i \prod_{sh.pt.j-h} (\psi_j \psi_h 10^M p_{jh}) \hat{p}_j, \tag{4.4}$$

which approximates the collision of object i with the debris of object j due to a chain of fragmentations along the shortest path between the network's node j and all other nodes h in the network Fig. 4.3.

As presented in [2], by removing some of the underlying assumptions, the previous for-

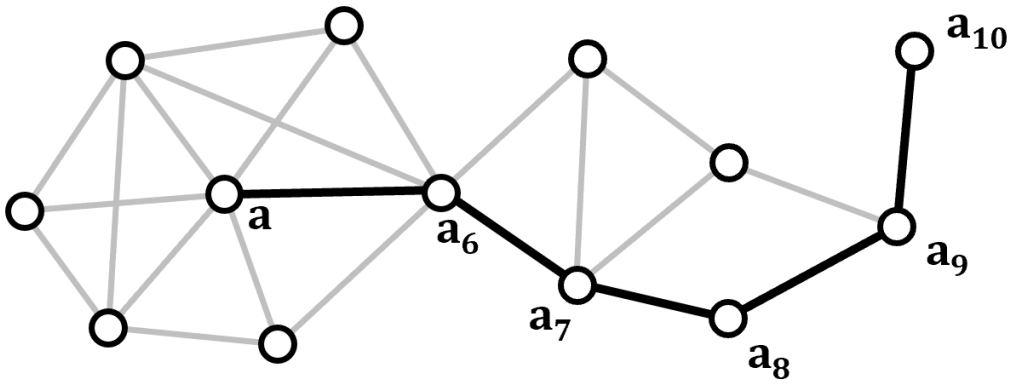

Figure 4.3: Visual representation of the third contribution, from [1].

mulation can be rewritten as a function of the sole network properties:

$$S^{(i)} = pD_i + p^2 C_i D_i (D_i - 1) + B_i p^{1/K_i}, \tag{4.5}$$

where the degree D, clustering coefficient C, betweenness B, and closeness K (which will be briefly introduced in Appendix A) are combined in a more compact formula.
For an in-depth discussion of the simplified model, its derivation, its meaning and interpretation, the reader is invited to refer [2].
The data processing, that focuses on simulating the evolution of space debris orbits for a set time, has been carried out on Fortran and Python. The data set used to perform the simulations comes from Space-Track, that provides both TLEs [59] and Conjunction Data Messages (CDMs) [60] of orbiting objects. Any of the two format can be used in order to generate the network and obtain the desired results. These data are analysed and lists of conjunction events are created.
The post-processing, that is what this research focuses on, is carried out on MATLAB. Here, all data coming from the processing part are used as inputs for the evaluations that follow. The list of conjunction events is used to create the graphs that are the base for every calculation and analysis that is subsequently carried out.

4.1. Processing

TLEs are composed of two lines of alphanumeric text that describe the orbital parameters of the related RSO. They need to be propagated for the selected time. The chosen method to do so is the Standard General Perturbations 4 (SGP4) [61]. While being based upon an approximate model which limits its applicability to spans of a few days due to the limited

accuracy, this propagator is entirely analytical, thus allowing for fast simulation times. The model still includes atmospheric drag, Earth's gravitational potential, luni-solar and planetary gravitational perturbations and direct Solar Radiation Pressure (SRP).
Then the propagated TLEs are filtered using a three-filter sequence, as suggested by [53]. The states of the orbiting population are filtered in order to find the pairs of RSOs that can create the actual list of conjunctions used to generate the graph.
All possible pairs of RSOs are analysed and filtered in sequence as follows:

- the 1^{st} filter compares the absolute minimum and absolute maximum of the two nodes of each pair with each other, in order to understand if there is a possibility of orbital intersections. This filter is an evolution of the one proposed in [62], where the perigee and apogee of the orbits where evaluated. If the difference between the largest minimum and the smallest maximum is less than a threshold distance, the couple passes to the next filter. Indeed, this means that there is a possibility of orbit crossing. In the opposite scenario, the pair could not undergo a crossing, since the smallest maximum would never get close enough to the largest minimum to possibly cause a collision.

- in the 2^{nd} filter, the MOID of the orbits are analysed. The MOID values are computed with sign according to the relative configuration of the two orbits, and its evolution in time is studied: any time a change in sign appears, there is a possibility of a conjunction, since the sign change represent an orbit crossing. If a change in sign appears, an orbital intersection is detected, and the pair of RSOs passes to the next filter.

- the 3^{rd} filter, finally, compares directly the Cartesian coordinates to detect if the distance at any time in the simulation is lower than a certain threshold. If it is, a conjunction between the two RSOs is finally detected: the pair passes the last filter and is included in the list final list of conjunctions.

A further explanation of the process, showing the main formulas and equations involved, is presented in Appendix B, while a scheme representing the process of the three-filter sequence is shown in Fig. 4.4.
CDMs, on the other hand, do not need filters or propagators, since they directly provide the conjunctions predicted in the simulation time under examination containing all the necessary information to compile a list of conjunctions (i.e. objects involved, epoch, distance, collision probability), ready to be analysed in the post-processing.

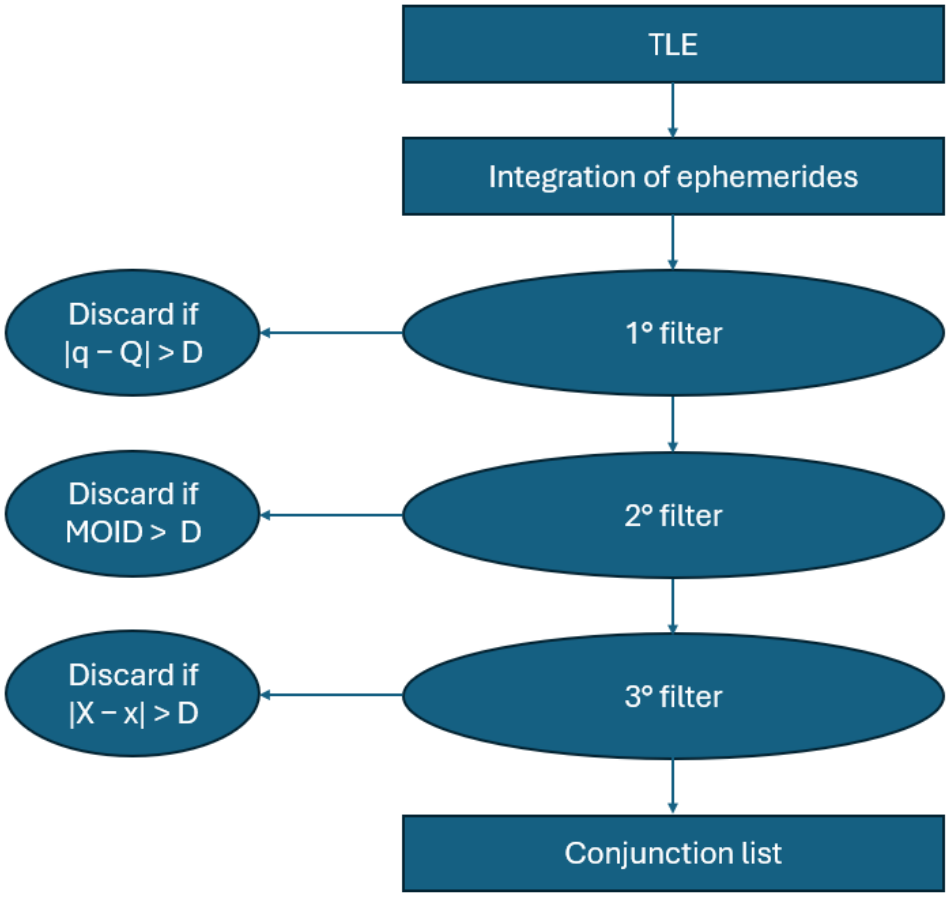

Figure 4.4: Scheme of the three-filter sequence.

4.2. Post-processing

The list of conjunction events inherited from the main processing, either from TLEs or from CDMs, is put at use during the post-processing. After a last filtering to remove repeated conjunctions involving the same objects, the RSOs in the list are embedded into a network which is simple, undirected, static, and free of self loops (meaning that no explosions are considered in the model [2]).

Built-in MATLAB functions are used to create and analyse the network. The adjacency matrix A is defined: for a network of n nodes, A is a $n \times n$ binary matrix, whose elements represent the edges of the graph, where $a_{ij} = 1$ if an edge connects nodes i and j (thus representing a conjunction between the two corresponding RSOs), otherwise $a_{ij} = 0$. By definition, matrix A is symmetric, since a conjunction between i and j implies that $a_{ij} = a_{ji} = 1$. These properties are used in order to create cycles that iterate the evaluation of the contributions for each node, by checking if a conjunction exists for each pair of nodes.

5 | Time-framed model

The risk metrics defined in [2] evaluates, for simplicity, each network under analysis as if every conjunction happened at the same time, thus ignoring the possible dependence of some impact probabilities from previous events. Introducing time dependence allows to represent the problem with more realism, while also improving the accuracy of the probability evaluations. Moreover, this could allow to extend the simulation to longer time spans without losing reliability in the results, since the length of each time window can be extended or shortened at will. Indeed, extending the simulation time in the static network means that events that may happen in distant moments in time are considered simultaneous. On the contrary, with the time-framed model the simulation time can be divided in more time windows, each of them being sufficiently short to allow accurate results. This being said, the chosen propagation method has to be accurate over longer periods of time in order to do so.
There are two ways to introduce time dependence in a network [63]. Temporal networks could be exploited, which could lead to the use of Bayesian networks, that are described by Stephenson [64]. The other possibility is to use static networks in order to simplify the representation of temporal networks. This method has been described by Holme, Saramäki ([63]). They suggest that, by analysing static networks at different time steps, a representation of time dependence can be obtained in a network. Indeed, doing this grants the possibility to analyse graphs that depict specific moments in time. Moreover, by using a high enough number of time windows, the series of static networks can represent the evolution in time of the RSONet approximating a temporal network.

5.1. New contributions

By following the model already introduced by Romano et al. [1] [2], introducing some variations, a time-framed model has been designed, where every contribution to the score at each time step carries by some dependence from previous time steps.
The contributions are evaluated differently in this work with respect to Romano, Carletti, Daquin [2] formulation. The differences are going to be explained subsequently.

The choice to divide the simulation time in different windows carries by the need of some adjustments to the formulation of the contributions. Thus, the new contributions C_1 and C_2 are subsequently thoroughly explained. For simplicity, this work ignores the third contribution, since the results from [2] showed that it is most times negligible with respect to the first two contributions.
The most visible modification clearly comes from the different approach to the problem that the two methods have, the static and the time-varying one.
A characteristic in common to the two contributions is indeed the presence of a term that accounts for the possibility of having a collision before the current time step. There is a new hypothesis added to the ones already explained in Chapter 4. The probability of an object i of colliding is evaluated as its probability of having a close approach with an object j at a certain time window, which is dependent on the probability of the i and j having fragmented at a previous time window. Indeed, the i can have a close approach with the j only if both of them have not collided before. This is visible in Eq. 5.1:

$$P(A|\overline{B}) = P(A)(1 - P(B)). \tag{5.1}$$

The probability $P(A|B)$ is the probability of the event A conditioned by the event B (the fragmentation of i depending on the collision of j and i not happening at previous time windows), $P(A)$ is the probability of A happening (the collision between i and j), while the probability $P(B)$ is the probability B happening (i.e. the probability of j fragmenting at a previous time window). This means that $(1 - P(B)) = P(\overline{B})$ is the probability that j has not collided before the current time step. With this hypothesis in mind, the two contributions can be presented.
C_1 is computed as follows (Eq. 5.2):

$$C_1^(i)(T_k) = \bar{p}_i(T_k) = \bar{p}_i(T_{k-1}) + \sum_j p_{ij}(T_k)(1 - S_i(T_{k-1}))(1 - S_j(T_{k-1})). \tag{5.2}$$

The contribution is now computed taking into account the previous time steps probabilities, that have an impact on following steps, tending to decrease the value of C_1, as explained before (Eq. 5.1). The idea behind this formulation is that a collision between two nodes could happen only if neither of the two has already been involved in a collision at a previous time step. This effect is represented via the terms in brackets in Eq. 5.2. There is a product between these two values, since the probability that has to be considered is that of none of the two events, i.e. the collision of i and j at previous steps, happening, with the events being independent. Thus, they need to be multiplied between each other (Chapter 3.2).

These terms are also the ones that introduce some sort of cross-connection between the two contributions. This is one of the main differences between this revised network and the original one. Indeed, in the work carried out by Romano, Carletti, Daquin [2], the contributions are all separate entities that are not connected in any way. Thus, they only contribute together to form the total score S, but do not directly interact between each other in any other way. The new terms in brackets result from the different nature of the time-famed risk metrics. The implementation of time dependence as a series of snapshots leads to the introduction of cycles, where each step is influenced by the previous ones. In particular, the score at previous steps is the responsible of diminishing the total value of C_1 and, as it is going to be shown subsequently, of C_2.
For the term C_2 a similar approach has been considered, with its value being determined through the Eq. 5.3:

$$C_2^i(T_k) = \tilde{p}_i(T_k) = \tilde{p}_i(T_{k-1}) + \sum_j S_b^{(j)} \hat{p}_{ij}(1 - S_i(T_{k-1})). \tag{5.3}$$

Here the second main modification becomes clear. The $\hat{p}_{ij}$ represents the probability of the object i of encountering a debris originated by the fragmentation of j, i.e. a debris coming from a debris cloud generated starting from j. The term $\hat{p}_{ij}$ has been evaluated in a completely new way, with two cases that exploit different formulas:

- If the possible conjunction causing a fragmentation of j belongs to the same time window as the close approach between i and j, the equation used is the following one:

  $$\hat{p}_{ij} = p_{ij}, \tag{5.4}$$

  since during the short enough observation period the debris cloud originating from j will remain very close to the latter object, as an approximation for a recent fragmentation.

- If the possible conjunction causing a fragmentation of j belongs to a previous time window, then a different equation has to be used:

  $$\hat{p}_{ij} = 1 - e^{-N}. \tag{5.5}$$

In Eq. 5.4, the probability of i colliding with a fragment of j is still the simple probability of i encountering j. This formula comes from the idea that, if the fragmentation of j happened at a close enough moment in time, i.e. the current time window, the debris cloud can still be considered as the single node j, since there has not been enough time for it to

disperse along the original orbit. In the second scenario, the fragmentation happened in a previous time window, thus several orbital periods have passed, allowing the spreading of the debris along a toroid in the region of the original orbit. The formula used comes from the paper written by Letizia, Colombo, Lewis [65]. The way this formula is created is going to be explained in detail in Chapter 5.3, together with a further explanation about the reasoning behind the choice of using the Eq. 5.5.
Moreover, any possible collision happening at previous time windows, that could create a debris cloud from node j, has to be considered. This means that the probability of the node i colliding with a debris coming from the debris cloud generated by j is dependent on the node j actually fragmenting. For this reason, the whole contribution is multiplied by the term $S_b^{(j)}$. A distinction has been created between the cases in which the fragmentation happens at the current time window and those in which the fragmentation happens before. In the first case the value of $S_b^{(j)}$ being considered should be $S_b^{(j)}(T_k)$, so the score of j at the current time step. Since there is the possibility that the score of the node j has not been evaluated yet, the score is in this scenario substituted by a value $S_b^{(j)} = 10^{-5}$, a value in line with the values of the largest scores that have been observed in the simulations, in order to be conservative. In the second scenario, with the fragmentation of j happening at a previous time step, the actual score of j at the previous time window $S_j(T_{k-1})$ has been considered.
C_2 value should not be diminished by the score of j at previous steps $S_j(T_{k-1})$, since the probability of a collision that may have caused a fragmentation of j in previous time windows has been considered inside the formulation of $S_j\hat{p}_{ij}$. Thus, the only factor diminishing the probability is $S_i(T_{k-1})$, with the same reasoning used for the first contribution (Eq. 5.2.

5.2. Simple example for a theoretical scenario

A simple example of how the risk metrics is intended to work when taking sequentiality of possible impacts into account, given the previously defined formulas, is here presented. The network in Fig. 5.1 is composed of 6 nodes and 6 links total. If the previously defined risk metrics was to be used to evaluate probabilities of collisions, there would have been no need to keep track of the order of events. In this case though, the order of appearance of links between the nodes is important in defining the scores. In order to present the main difference between this time-framed risk metrics and the original method, the probability $\bar{p}_i$, representing the first contribution, is here evaluated for each node i at the different time steps T_j.

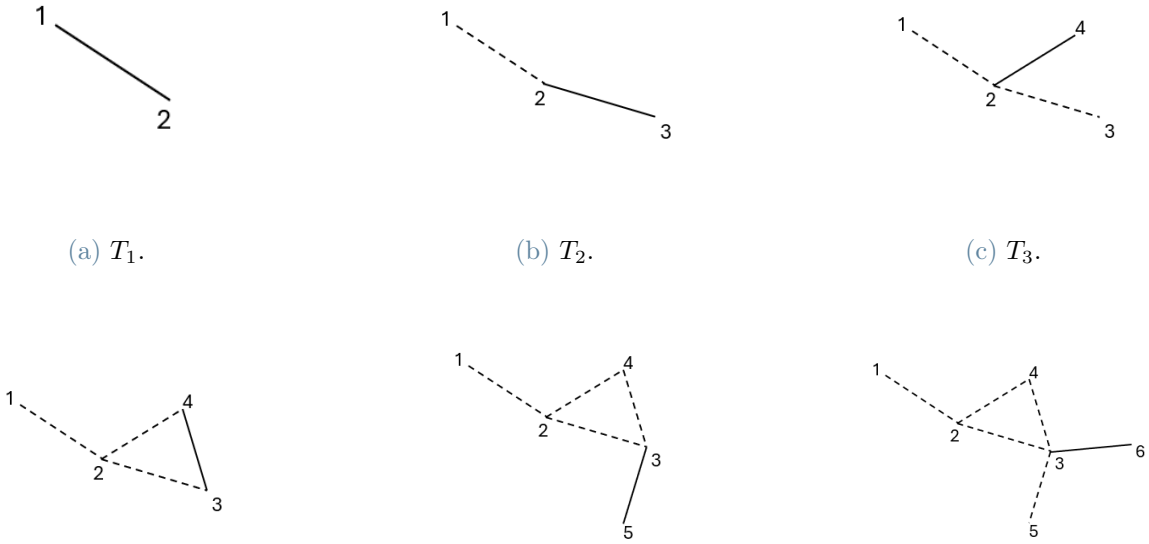

(a) T_1. (b) T_2. (c) T_3.

(d) T_4. (e) T_5. (f) T_6.

Figure 5.1: Network used for example purposes.

- T_1 (Fig. 5.1.a)
  1. $\bar{p}_1(T_1) = p_{12}$
  2. $\bar{p}_2(T_1) = p_{12}$
- T_2 (Fig. 5.1.b)
  1. $\bar{p}_1(T_2) = \bar{p}_1(T_1)$
  2. $\bar{p}_2(T_2) = \bar{p}_2(T_1) + p_{23}(1 - \bar{p}_2(T_1))$
  3. $\bar{p}_3(T_2) = p_{23}(1 - \bar{p}_2(T_1))$
- T_3 (Fig. 5.1.c)
  1. $\bar{p}_1(T_3) = \bar{p}_1(T_2)$
  2. $\bar{p}_2(T_3) = \bar{p}_2(T_2) + p_{24}(1 - \bar{p}_2(T_2))$
  3. $\bar{p}_3(T_3) = \bar{p}_3(T_2))$
  4. $\bar{p}_4(T_3) = p_{24}(1 - \bar{p}_2(T_2))$
- T_4 (Fig. 5.1.d)

1. $\bar{p}_1(T_4) = \bar{p}_1(T_3)$
2. $\bar{p}_2(T_4) = \bar{p}_2(T_3)$
3. $\bar{p}_3(T_4) = \bar{p}_3(T_3) + p_{34}(1 - \bar{p}_3(T_3))(1 - \bar{p}_4(T_3))$
4. $\bar{p}_4(T_4) = \bar{p}_4(T_3) + p_{34}(1 - \bar{p}_3(T_3))(1 - \bar{p}_4(T_3))$

- T_5 (Fig. 5.1.d)
  1. $\bar{p}_1(T_5) = \bar{p}_1(T_4)$
  2. $\bar{p}_2(T_5) = \bar{p}_2(T_4)$
  3. $\bar{p}_3(T_5) = \bar{p}_3(T_4) + p_{35}(1 - \bar{p}_3(T_4))$
  4. $\bar{p}_4(T_5) = \bar{p}_4(T_4)$
  5. $\bar{p}_5(T_5) = p_{35}(1 - \bar{p}_3(T_4))$
- T_6 (Fig. 5.1.d)
  1. $\bar{p}_1(T_6) = \bar{p}_1(T_5)$
  2. $\bar{p}_2(T_6) = \bar{p}_2(T_5)$
  3. $\bar{p}_3(T_6) = \bar{p}_3(T_5) + p_{36}(1 - \bar{p}_3(T_5))$
  4. $\bar{p}_4(T_6) = \bar{p}_4(T_5)$
  5. $\bar{p}_5(T_6) = \bar{p}_5(T_5)$
  6. $\bar{p}_6(T_6) = p_{36}(1 - \bar{p}_3(T_5))$

The example previously presented does not include the possibility of second degree linked nodes appearing at the same time step. However, the possibility exists, and has been considered in the code designed during this research.
This example meant as a simple way to notice the differences in the formulation of the first contribution between a time-framed and a static network. In order to better highlight it, an example of how the $\bar{p}_i$ would have been evaluated, in the same scenario, is presented right away. Let us now consider the following simple figure (Fig. 5.2) as the network under study. This network is analogue to the one in Fig. 5.1. The difference between the two examples is due to the fact that, while in the first case the various close approaches were happening in different time windows, in this case it is as if they were all happening at the same time, in the same way it would have been with the metrics presented by Romano et al. ([1] [2]).

1. $\bar{p}_1 = p_{12}$

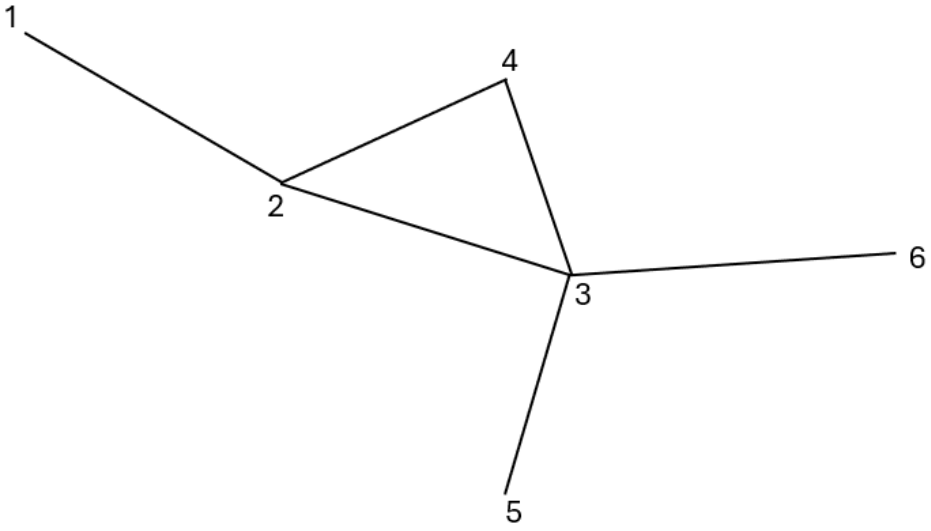

Figure 5.2: Network used for example purposes.

2. $\bar{p}_2 = p_{12} + p_{24} + p_{23}$
3. $\bar{p}_3 = p_{23} + p_{34} + p_{35} + p_{36}$
4. $\bar{p}_4 = p_{24} + p_{34}$
5. $\bar{p}_5 = p_{35}$
6. $\bar{p}_6 = p_{36}$

What can be noticed here is that the probabilities are not diminished by any value. Indeed, the fact that all the conjunctions are evaluated in a single time window makes it so that the probability of a conjunction happening does not depend on the fact the the nodes involved are still intact at the time of close approach, since the network does not track down the epochs of conjunctions.
This simple example allows to show the impact that time dependence has on the network. The contribution is diminished by the probability that the node inherits from the previous time windows. Indeed, the node can only fragment at a certain time if it has not already fragmented at previous time windows.
In this example, the factor contributing to diminishing the value of $\bar{p}_i$ is just the $\bar{p}_i$ of previous time windows, since the $\tilde{p}_i$ has not been evaluated for this scenario. However, the calculations in this work do consider the total score S_i of a node at previous time steps as a factor that limits the growth of the contribution between successive temporal intervals.

5.3. Evolution of debris clouds

Debris clouds are a major problem in terms of identification and prediction for STM purposes. They are generally caused by catastrophic collisions between two large objects, or a large object and a smaller one. For simplicity, we assume that an accident between two small enough RSO, which implies the $\phi = 0$ for the two nodes, cannot generate a cloud. This assumption comes from the first iteration of the model, as already addressed in 4.
A solution for the evaluation of the collision probability in presence of debris clouds is given by Letizia, Colombo, Lewis [65]. In the aforementioned paper, debris clouds are considered as a fluid, and their evolution in time is studied by analysing the density of the clouds, highlighting the effects of atmospheric drag on their behaviour. A continuum approach is considered, with orbital parameters used in order to build a continuous density function. This is later used to evaluate the evolution of the debris cloud and its dispersion, on a long-term scale. The model thus neglects the effects of latitude on the motion of the cloud, since it mainly affects the short-term evolution.
Another study, expanding and further advancing this method, has been carried out by by Giudici, Trisolini, Colombo [66], analysing the non-linear dynamics of debris clouds. Keplerian elements and area-to-mass ratio are exploited to describe the propagation of clouds of fragments. This method, too, can offer precise results on a medium term timewise, consisting of a few years.
In the context of this work, a short period is considered that of a few orbits, up to a couple of days. Then a large one would be a time span of more than a month, which means that the everything in between would be considered a medium time period.
For the purpose of the thesis, the propagation has to be carried out on a medium term. The aforementioned method [65] can still be considered as a base and then modified accordingly to the needs of the time-framed risk metrics under study, in order to evaluate shorter time periods behaviour of debris clouds.
Going more in depths into the topic, the evolution of a space debris cloud can be summarised and divided in three main parts:

- Ellipsoid (Fig. 5.3.a), the moment right after the fragmentation. The cloud is still dense and compact, but it is already starting elongate along the direction of motion on the orbit. In this research, this condition is valid in the short term.
- Toroid (Fig. 5.3.b), after a few orbits. The cloud has dispersed along the whole orbit because of the different energy the fragments retained after the collision. In this work, this model applies to the medium term evaluations.
- Band (Fig. 5.3.c), after a few months. Perturbations cause the spread of the frag-

ments in a band around the Earth, that is limited in latitude by that of the original orbit followed by the debris cloud. All the orbital perturbations have an effect in spreading the cloud. This condition has not been considered in this version of the model, since the simulations were way shorter.

The whole process can be visualised properly in Fig. 5.3, with each step of the evolution of the cloud highlighted in the image. The first two phases have been utilised in this

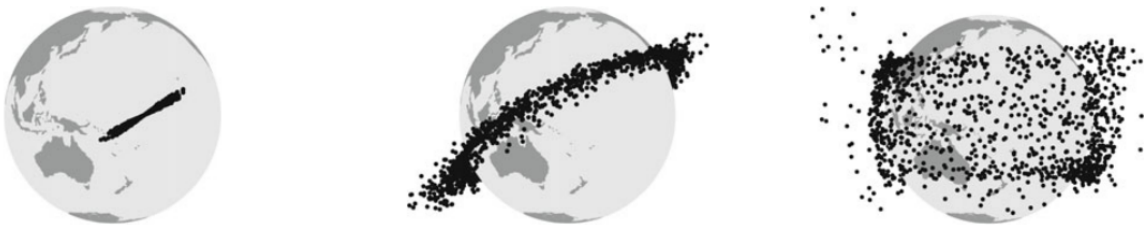

Figure 5.3: Evolution of the debris cloud in its three steps, from [37].

work, while the third one has been neglected, due to the brief time spans that are under consideration in this work (up to a few weeks), which are insufficient for the formation of the band. In this thesis Eq. 5.5 has been used, that is derived from [65]. That equation is related to the toroid phase just described. An in-depth explanation about its evaluation is here provided.
First, a few data are needed. Let us name the nodes. The nodes j and k are the ones involved in the generation of the debris cloud, with j being the biggest one. The node i is then the one that has a close approach with the debris cloud. The needed data, coming from the simulations, are the following ones:

- Position vector of i at the epoch of conjunction r_i
- Position vector of j at the epoch of conjunction r_j
- Impact velocity Δv_{jk}
- Mass of j m_j
- Mass of k m_k
- Cross section area of i σ

The first three pieces of data come directly from the graphs used for the simulations. The masses and the area are connected to their respective nodes through the graph, and they are taken from the CelesTrak catalogue.

After having evaluated all the preliminary data, the NASA BUM ([32]) has been exploited. By taking as inputs Δv_{jk}, m_j and m_k, the number of fragments N_f and the relative velocity vector of the fragments with respect to j Δv_{jk} are calculated. These are then used in order to find the velocity vector of each fragment v_{jk}. Then the perigee and apogee of each fragment r_{pjk} and r_{ajk} are evaluated, through the semi-major axis a and the eccentricity e derived from the transformation from cartesian coordinates to keplerian elements. These are later used in order to estimate the thickness Δx of the toroid, that has been approximated to a tube of fixed diameter. This is used to calculate the time Δt needed by the node i to pass through the toroid. This time also depends on the number of orbits the RSO completes in a single time window, that in turn depends on the length of each time window.
Finally, the last pieces of data needed for the evaluation of p are calculated. The process, described in [65], is represented followingly:

1.
$$n = \frac{1}{4\pi r_j a\sqrt{e^2 - (\frac{r_j}{a} - 1)^2}}. \tag{5.6}$$

2.
$$F = n\Delta v. \tag{5.7}$$

3.
$$N = F\sigma\Delta t. \tag{5.8}$$

4.
$$p = 1 - e^{-N}. \tag{5.9}$$

The variables here involved are a value of spacial density n, a measurement of the flux F and the average number of collisions over time N. By these means, the probability p has been evaluated and exploited in this thesis.

5.4. Main post-processing modifications

Since new formulas and concepts have been included in the formulation of the time-framed risk metrics, a few comments are needed. The post-processing part described in Chapter 4.2 in the original version of the method have been re-utilised, with some modifications and additions.
In order to create the adjacency matrices for the different time windows, a series of mask

matrices have been defined. Each of them has been derived from the complete adjacency matrix that would have been used for the static network. The scope of the mask matrices is to "hide" the non-null elements of the adjacency matrix not belonging to their related time window. Each of them is a binary matrix with the same dimensions as the complete adjacency matrix that defines the static network. However its elements are defined as 0 or 1 depending on the time window it belongs to. Calling M^k the mask matrix defined for the k^{th} time window, if a conjunction between objects i and j occurs during said window then $M^k_{ij} = 1$, otherwise $M^k_{ij} = 0$. Calling A the complete adjacency matrix and A^k the one defined for time window k, $A^k = M^k \circ A$, where $\circ$ denotes the point-wise product of two nxn matrices such that $A^k_{ij} = M^k_{ij} \times A_{ij}$. This way we can define the adjacency matrices for all subnetworks, thus accounting for the change in time. Moreover, in order to keep track of past events, needed for the evaluation of C_2, matrices A^k_{TOT} built as a sum of the mask matrices M^k up to the last time window considered before the current one. Their use is going to be explained in Chapter 5.5.

5.5. Implementation

A clarification about the main changes applied to the code is here presented. They revolve around the new contributions and how they have been implemented. These contributions need to be evaluated in the same loop at each time window. Indeed, their evaluation needs to use the total score at the previous time window. A few cycles are needed in order to calculate their values, since some checks need to be performed. These checks are needed in order to make sure to be able to correctly relate a conjunction to the right nodes.

Regarding the second contribution, both the current and the previous time windows have been considered at each step for its evaluation. If i is the object for which the score is being evaluated, j is the one that fragmented on its orbit through a collision with a third object k, generating a debris cloud. In this scenario, each evaluation has been carried out by considering the probability of a conjunction between the objects i and j at the current time step, while evaluating the fragmentation of j caused by conjunctions between j and k at previous time steps. This differentiation in the time windows considered has been carried out by exploiting multiple mask matrices at the same time window. The one related to the current time step A^k has been used to assess the probability of conjunction between nodes i and j, while the one related to previous time steps A^k_{TOT} has been exploited in order to evaluate the probability of a fragmentation of j, i.e. a collision between j and any node k. It would be possible to modify the number of time windows after which a the debris cloud is considered dispersed as a toroid by building A^k_{TOT} differently. The change

needed would be to write it as the sum of the mask matrices up to a certain time $k - a$, with a being the number of time windows that have to be considered before the evolution of the debris cloud into toroid happens.
Moreover, when changing the number of time windows, the number of orbits for which the Δt, used for the evaluation of the evolution of the debris cloud, is multiplied changes accordingly. The number of orbits per day that has been used is 12. That is multiplied by a factor b, that indicates the number of days per time window.

6 | Results and considerations

The analysis has been carried out on a simulation referring to the whole month of May 2023, starting on 1^{st} of May, 12:00 p.m., in order to compare the results obtained with the static model with the ones obtained using the time-framed model. The results that are going to be presented have been obtained with 15 time windows, thus meaning that each of them covers a time interval of 2 days.

A comparison between the static RSONet and the networks per each time window created through the time-framed risk metrics can be done. It is possible to notice the difference in how big the single components are in the two versions. The network in Fig. 6.1 contains some large components with many nodes in them. This is caused by the fact that, without any filter related to the time window of conjunction, any close approach happening during the whole simulation time is considered when creating the network. On the other hand, when considering the time-framed network, components tend to get

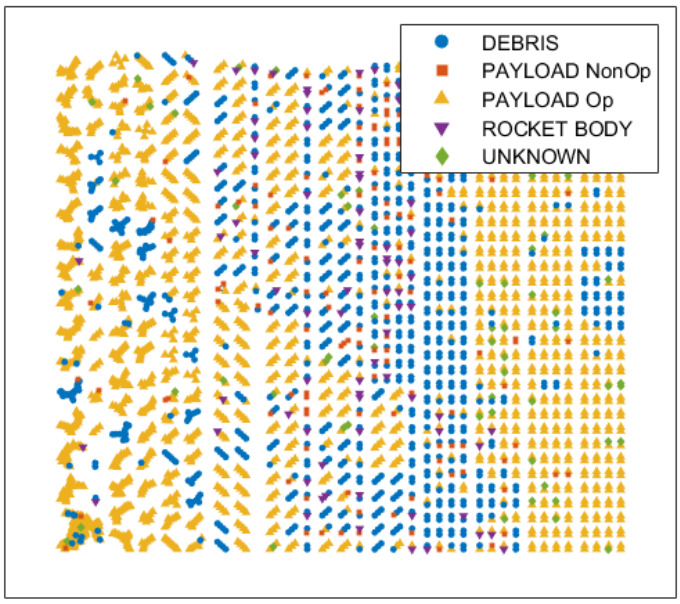

Figure 6.1: Static RSONet along the whole simulation time.

smaller, since the number of conjunctions happening in each time window is bound to be lower than the total number of conjunctions considered along the whole simulation time. A visual representation of one subnetwork, evaluated at the 1^{st} and the 15^{th} time window can be seen in Fig. 6.2.

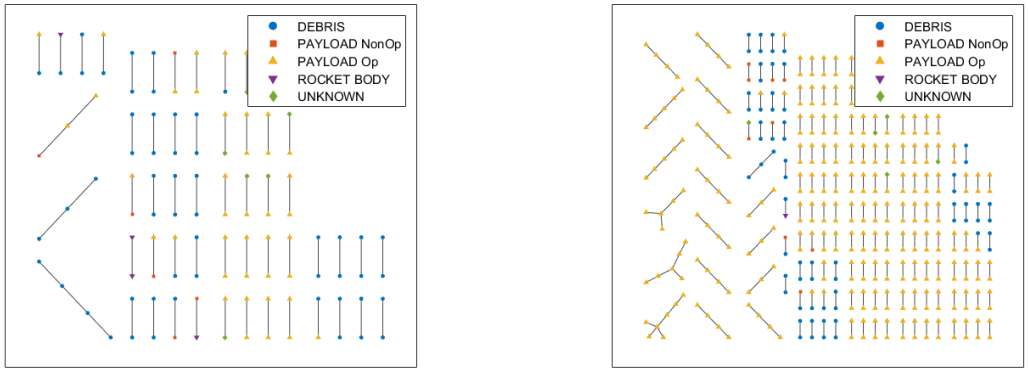

(a) 1^{st} time window.

(b) 15^{th} time window.

Figure 6.2: Time-framed network evaluated in two different time windows.

A clearer idea of how many connections are present in these two versions of the RSONet, let us zoom in on the largest components in the networks. Fig. 6.3 allows to compare the biggest component of the static RSONet with the biggest component of a single window in the time-framed network. This comparison highlights even better the difference between the number of nodes and edges a component can have, considering the same simulation time for the two conjunction lists. By increasing the interval considered in each time window, their components are bound to grow, since progressively more conjunctions are going to happen at the same time step.

An interesting comparison can be made between the time-framed score S evaluated at final step using 15 time windows, the static score, here called S_{st}, and a score evaluated using the new contributions, but considering just one time window as in the scalar case S_b. This means that, for evaluating S_b, none of the factors $(1-S^{(i)}(T_{k-1}))$ and $(1-S^{(j)}(T_{k-1}))$ have been considered, since no previous time steps are present. Moreover, no checks have been made regarding the epochs of the collisions, since they are considered as if they all happen at the same time.

This comparison can allow us to notice how each modification to the static network has

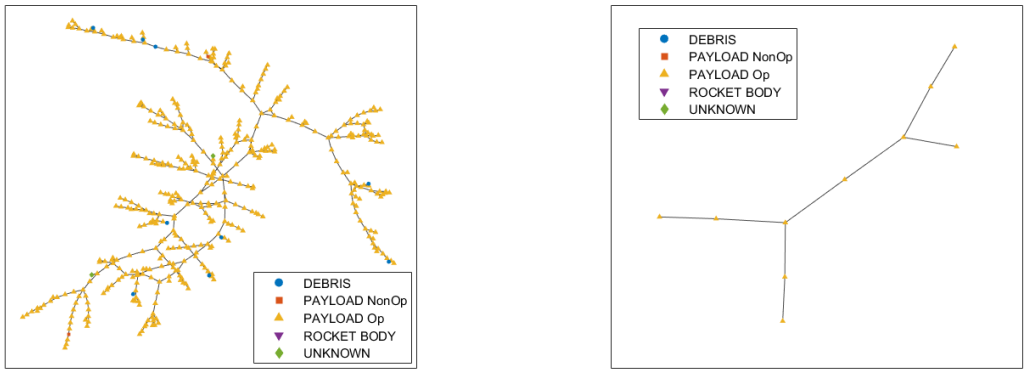

(a) Largest component of the static network.

(b) Largest component between all the time windows of the time-framed network, from the 9^{th} time step.

Figure 6.3: Comparison between the largest components.

caused significant changes in the values of the scores. The 10 highest scores for each case are shown in Tab. 6.1. What can be noticed is that the values of the highest scores

10^{-5} x	S	S_{st}	S_b
	3.07565	5.56454	11.5802
	2.85263	4.91493	8.08123
	2.66426	4.89338	6.76522
	2.64559	4.77196	6.59334
	2.43424	4.70032	6.42251
	2.35045	4.44003	5.97934
	2.17286	4.00497	5.70529
	2.05316	3.96789	5.52563
	2.03498	3.92383	5.35057
	1.93695	3.87390	4.70333

Table 6.1: 10 highest scores for S, S_{st} and S_b.

for the static network are higher than the highest scores in the time-framed network. This difference is due to some terms introduced in the new score, more precisely to the dependence that exists between a collision at a certain time step and the missed collisions at the previous ones. To explain it in a clearer way, the terms $(1 - S^{(i)}(T_{k-1}))$ and $(1 - S^{(j)}(T_{k-1}))$ in the time-framed score contribute to decrease the values of the contributions

at each time step, resulting in lower scores than the static case. The other peculiarity to be noticed is the higher values of the scores evaluated through the new contributions, but using a single time window, as done in the static network. The values of S_b are much higher than the respective highest values of S and S_{st}, meaning that the modified contributions

Another interesting result obtainable from the analysis of the time-framed network is the evolution over time of the score of some components. In Fig. 6.4 it is possible to see the trend of the score S for some selected nodes, compared to the maximum value of S_{st}. The involved nodes are N_1 (maximum S at time step 2), N_2 (maximum S at time step 6), N_3 (maximum S at final step), N_4 (maximum C_2 at final time step), N_5 (minimum S at final time step) and $N6$ (maximum S_{st}).

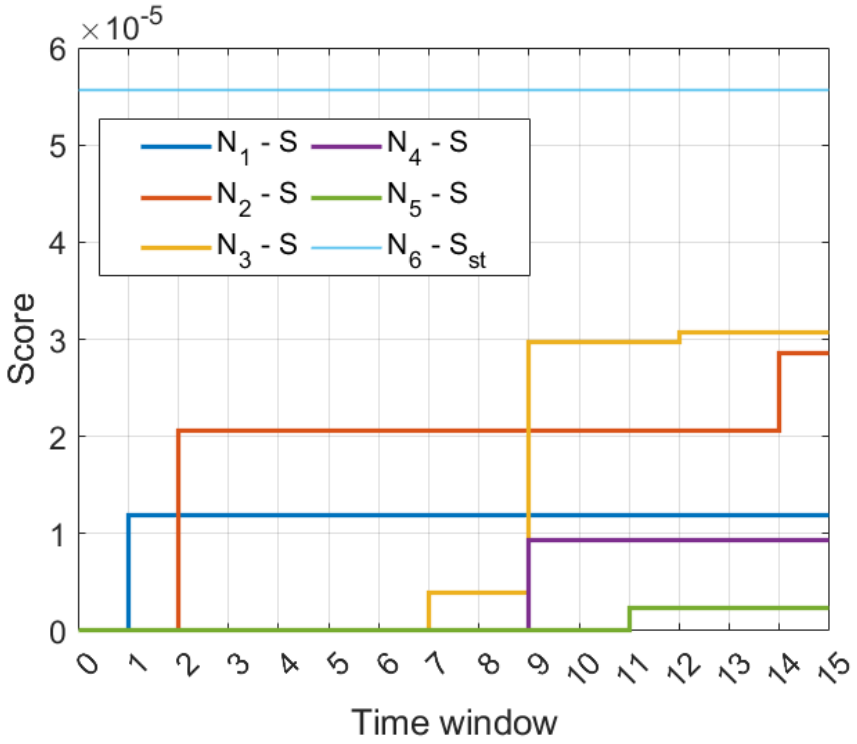

Figure 6.4: Trend of S for 5 selected nodes, compared to the maximum S_{st}.

A couple of interesting details can be noticed here. First, even if a node has the highest score at the end of the simulation time, it does not necessarily mean that it also has the highest score along the other time windows. Another interesting fact is that, as predictable, the main contribution in the score is C_1. Indeed, its order of magnitude is usually twice the order of magnitude of C_2 for each node, due to how they are evaluated. Indeed, the physical explanation is straightforward. While C_1 depends on the probability of a collision between two objects i and j, C_2 depends on the probability of collision of the

same two objects i and j, but also on the one related to the second object j and any third object k, thus decreasing its value. Then it is possible to notice once again the difference between the maximum S and the maximum S_{st}, with the latter being much higher than any score S evaluate with the time-framed model.
The trend of the scores shown in Fig. 6.4 is also presented in Tab. 6.2, where the values of S in a few key time windows are reported. Then also the trend for C_1 and C_2 can be shown in Tab. 6.3 and 6.4.

	$S(t_2)$	$S(t_7)$	$S(t_{15})$
N_1	$1.19375\text{x}10^{-5}$	$1.19375\text{x}10^{-5}$	$1.19375\text{x}10^{-5}$
N_2	$2.05316\text{x}10^{-5}$	$2.05316\text{x}10^{-5}$	$2.85263\text{x}10^{-5}$
N_3	0	$3.89189\text{x}10^{-6}$	$3.07565\text{x}10^{-5}$
N_4	0	0	$9.31644\text{x}10^{-6}$
N_5	0	0	$2.32069\text{x}10^{-6}$

Table 6.2: Trend of S, along some of the considered time windows, related to the nodes in Fig. 6.4.

	$C_1(t_2)$	$C_1(t_7)$	$C_1(t_{15})$
N_1	$1.19375\text{x}10^{-5}$	$1.19375\text{x}10^{-5}$	$1.19375\text{x}10^{-5}$
N_2	$2.05317\text{x}10^{-5}$	$2.05315\text{x}10^{-5}$	$2.85263\text{x}10^{-5}$
N_3	0	$3.89189\text{x}10^{-6}$	$3.07565\text{x}10^{-5}$
N_4	0	0	0
N_5	0	0	$2.32069\text{x}10^{-6}$

Table 6.3: Trend of $C1$, along the considered time windows, related to the nodes in Fig. 6.4.

	$C_2(t_2)$	$C_2(t_7)$	$C_2(t_{15})$
N_1	0	0	0
N_2	0	0	0
N_3	0	$2.10240\text{x}10^{-14}$	$6.96390\text{x}10^{-13}$
N_4	0	0	$9.31644\text{x}10^{-6}$
N_5	0	0	$3.85079\text{x}10^{-14}$

Table 6.4: Trend of C_2, along the considered time windows, related to the nodes in Fig. 6.4.

These tables show how the main contribution to the score is always the C_1, while C_2 is

generally some order of magnitude smaller. This is due to the fact that, for C_2 to be evaluated, two conditions have to be met: the conjunction between i and j at time k, and the fragmentation of j in a previous time window. Indeed, even though the node N_4 has the highest value of C_2 at the final step, its score S is much smaller than that of node N_1, that has the highest score at the final step. The value of C_2 is also the one that oscillates the most between different nodes, as one can notice when looking at its value for the nodes N_4 and N_5 at the final step.
Finally, a characteristic of the time-framed model has to be mentioned. The nodes of the network for which the score is non null are, in general, different with respect to the ones for which the score is non null in the static RSONet. This means that, for example, the node related to the highest score S is, a priori, different from the one related to the highest S_{st}.
Possible causes may derive from the division of the simulated time in time windows, that may eliminate a few edges with respect to the static RSONet, and the modifications that the contributions have undergone in the new formulation. The reasons behind this behaviour have to be further analysed in future works.

7 | Possible applications, conclusions and future developments

The study of space environment becomes progressively more important as the space industry continues to grow. The number of space debris in orbit, as already analysed in Chapter 1, is exponentially growing, leading to an environment that is bound to become oversaturated in a short time.
The research presented throughout this thesis, with the purpose of improving the accuracy of the already existing method presented by Romano et al. ([1], [2]), aims at adding another, more refined tool to the list of methods and models described in Chapter 2.1.
Many applications can be thought about that can be faced through the use of this time-framed risk metrics. All of them may be decisive in order to tend towards the ambitious goals of reducing the number of space debris already in orbit and decreasing the currently worrying rate of production of new debris.
A distinction can be made between these applications, with further explanations and ideas following subsequently:

- Theoretical applications, mainly the study of space environment health and conditions.
- Practical applications, that may present major differences between each other, but they all aim to reduce or possibly stop the growth of space debris number in orbit. They vary significantly in terms of functions and purpose, from ADR to CAM, but they all need accurate data regarding the space environment in order to be utilised.

A distinction has been highlighted, but these applications are going to be explained in further detail in the following Chapters 7.1 and 7.2.

7.1. Theoretical applications

Researches on space environment health have been performed in numerous different ways, usually exploiting the existing models of the likes of the ones described in Chapter 2.1. They mainly focus on the analysing the history of space debris, the main collisions that happened in the past and the possible future evolution of the space environment. An example could be the many studies that focused on the infamous Iridium-Cosmos collision, which studied the historical event in different ways in order to retrieve useful information on how the impact occurred, what could be done in order to avoid it, in which ways it affected the space environment in the following years and how would it be, or have been, possible to reduce the aftermath on the rest of the space population. A few examples on this case can be brought to attention.

A couple of studies have already been discussed. The analyses performed by Pardini, Anselmo ([3], [30]) have already been discussed in Chapter 1 and 2. They used the same method in their two iterations of the analysis on the Iridium-Cosmos collision, with the use of SDIRAT in order to assess the flux of debris involved in the collision. The main results of the study are related to the increase in the flux of debris by a high margin in the interested area, that testifies the impact the collision had on the rest of the space population.

Another interesting research has been conducted by Kelso [67], who carried out an analysis on the Iridium-Cosmos collision, by studying the previsions and simulations of the events that led to the impact. These analysis where conducted through Satellite Orbital Conjunction Reports Assessing Threatening Encounters in Space (SOCRATES), a service provided by CelesTrak that gives information about possible conjunctions over the coming week. An interesting representation of the conditions in 2009, when Kelso studied the collision, of the debris cloud originated from the event can be seen in Fig. 7.1.

The time-framed model can offer itself as a new tool to be used to analyse future developments in space environment, mainly on the short term. Since this method has been designed to work in a short temporal range, it is not actually suited for long term simulations.

This being said, it has been designed to exploit data catalogues coming from Space-Track, and the catalogue offers historical TLEs, that could be useful to analyse important and impactful past events. While still not suited for long term analyses, meaning it could not be easily used to retrieve the full consequences of a certain past occurrence, it can be utilised to assess the situation that led to the event under study, and analyse the space environment situation at that time, providing useful comparison to the current situation. Anyway, this method may probably prove more useful for the next applications that are

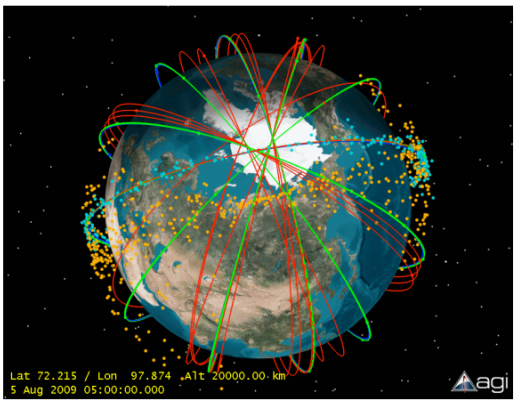

Figure 7.1: Representation, dated 2009, of debris cloud generated by the Iridium-Cosmos collision, from [67].

going to be presented in Chapter 7.2.

7.2. Practical applications

Possible practical applications differ in many ways between each other, in how they face the problem of space debris, the technologies they use and possible risks they may introduce.
In any case, the use of a method to understand the probabilities of collision of RSO can be useful in order to understand the best route to lower the risk for objects in orbit, or to directly remove debris from LEOs.
ADR is one of the possible practical applications that could effectively reduce the number of debris in orbit. In order to do so, a few steps are required, that pose important challenges to the space industry, both technical and political. The main technical problems are related to detection, capture and de-orbiting of the debris, as stated by Ansdell [68]. The technical challenges are still important, with the first mission designed to demonstrate a recovery of a RSO being the ClearSpace-1 [15], already cited in Chapter 1 and planned for 2028. Anyway, the contribution of ADR to the mitigation of the space debris problem may prove fundamental.
The model presented throughout the thesis could be useful in order to select the most appropriate targets for removal. Indeed, debris can be ordered according to their score at the various time steps, and this could be useful in two ways, both in understanding which are the best targets and which window may be the best one to perform the removal action. Let us consider, for example the node with maximum score at the last time window analysed in the simulation. That node would be a good target, since it has the highest

probability of collision throughout the whole simulation time. With the time-framed risk metrics, knowing the score at each time window could offer a second advantage. By tracking the score of the targeted node at the various steps, it would be possible to understand which window could be the most suited to perform the removal. That would be the one in which the score does not change with respect to the previous step, since the node would not face any close approach with other RSO in that time window. This would offer safer conditions for the ADR to be performed. If such window does not exist, meaning that the node in question could theoretically undergo a collision at any of the chosen time steps, two possibilities would still be in play. It would be possible to reiterate the simulation, increasing the number of time windows in which the simulated time is divided into, in order to possibly find a window in which the score does not actually increase. A problem in this case could be that the selected time window may become to short to actually be safely usable. The second possibility would be to simply find the time step at which the increment with respect to the previous evaluation is the smallest one. In this case the ADR could still be performed, with the downside of having a possibility of collision in that time window, either between the the two RSO already in orbit or between the mean selected to perform the removal and one of the debris possibly involved in a close approach at that time step. In any case, a trade-off between the risks involved in performing the removal and or leaving the targeted debris in orbit shall always be considered. Further considerations on this application are offered in Chapter 7.4.

Another possible practical application could be related to CAM. They are performed any time a risk of collision and its related probability, between an active spacecraft and another RSO exceeds the acceptable level [69]. They can be performed in various ways, such as low-thrust CAM, optimised manoeuvres that can allow the spacecrafts to minimise the needed Δv.

The model presented in this research may be applied to this field. Indeed, it is possible to isolate a specific node in the network and analyse only its conjunctions along the simulation time. The ability to target the RSO that contribute to the score of the spacecraft one is focusing on allows to understand when a manoeuvre should be performed in order to avoid the close approach. Moreover, this model could still be used for Just-In Time Collision Avoidance (JCA). These kind of manoeuvres, as specified by Bonnal et al. [70], are performed close to the predicted collision, thus the fact that the model currently simulates over a short time period would not be a minus.

Taking now into consideration the insertion of new spacecrafts into orbit, a problem that is likely to become progressively more impactful in the future, seeing the trends, is that of mega-constellations of satellites being launched in LEOs. Indeed, the launch of large constellations is growing in the last years, and it poses some new challenges to the preser-

vation of the space environment health [22]. Starlink and OneWeb are just two of the projects that already launched mega-constellation of satellites in orbit. Their impact on space environment is already important, and can only worsen with the addition of new satellites to the already existing mega-constellations, or the design of completely new ones [71]. Many researches focus on understanding the best methods to deploy mega-constellations, such as Sung, Ahn [72] or Di Pasquale et al. [73], with minimisation of costs or duration of the deployment being the main topics under study. This being said, an analysis on the launch phase could bring about useful information. It would be possible to compare two different deployment strategies, in order to assess the risk involved and which could be the safer option. An example of this application could be that of analysing the launch of 60 satellites at the same time, comparing it to two launches of 30 satellites each.

Finally, mission analysts could make use one of the time-framed risk metrics in order to safely plan their missions, e.g. the insertion trajectories or orbit change manoeuvres. By analysing the scores of RSO, it would be possible to find out which ones have the highest scores at a certain time. Then, by studying the evolution of their orbits, it would be possible to single out the epochs and the positions at higher risk of impact. Thus, possible countermeasures could be taken. This application would largely benefit from diminishing the duration of each time window, in order to more reliably connect the time step with the highest score increment and their position at that same time step. Clealry this could be useful also in EOL planning, in order to perform the necessary manoeuvres as safely as possible.

7.3. Conclusions

A model that analyses the RSONet at several time steps has been presented. This time-framed model exploits the main concepts of the RSONet designed in [2], improving it by adding time dependence. These improvements allow the model to be suitable for the applications presented in Chapters 7.1 and 7.2.

Modifications have been brought to the contributions used in the static model, with new hypotheses and formulations. The simulated time has been divided in several time windows. This allowed the score S at each time step to affect the score at the following steps. A different model to represent the evolution of debris clouds has been implemented, exploiting the NASA break-up model and the model developed by Letizia et al. [65]. This modifications allowed to represent the after-effects of fragmentations in a more realistic way.

The comparison between the static and the time-dependent score has highlighted the

general reduction of the values obtained through the time framed model. This result is consequence of the introduction of the terms that take the probability of fragmentation of a RSO at previous time steps into account, and it shows how introducing time dependence allows to analyse debris collisions considering the conditionality of the impacts, adding another layer of realism to the model. Moreover, the model can work over longer simulation times, if the propagation method allows it, as explained in Chapter 5.

7.4. Future developments

The model could undergo various processes in order to be improved in different areas. A possibility could be to use a propagation method that allows to accurately propagate the TLEs over longer periods of time. This could allow to increase the accuracy of the model itself on longer simulation times, in order to be more reliable for some of the applications presented in Chapter 7.2. For example, this improvement could help in programming actions of ADR more ahead of time, since some time is needed in order to actually perform such action. It could also offer more feasible time windows where the risk of encountering other debris while performing the removal is the lowest possible.
Also the other applications could benefit from this improvement. CAM and mission analysis would make a better use of this model by being able to perform simulations over a larger span, for reasons similar to the ones just presented. The possibility to plan in advance usually relates to being able to design more efficient manoeuvres. This then translates into saving propellant and thus reducing the cost of such manoeuvres, while also increasing the possible operational time of the satellite, that would have more propellant stored for other CAM or regular manoeuvres for orbit change or adjustment.
This action on the model would need to introduce the third stage of the debris cloud evolution, described in Chapter 5.3. The creation of a band surrounding the Earth would indeed become important over longer simulation times.
An interesting development could be the creation of an actual risk index, that associates each score with a risk level. A division of the near-Earth space environment in shells and sectors could be created, and a way to associate the conjunctions and the sectors in which they happen could be found. This could offer a more easily and quickly recognisable index that could show which sectors are associated with the lowest risks of collision in any simulated time window.
Moreover, possible improvements to the code may lead to faster simulations, decreasing the computational cost of the model, thus making it more efficient. There is also a possibility of adapting it to the use of CDMs, in order to have the possibility to choose between the two data sets. Finally, the probabilities of explosions could be inserted in

the simulations, thus adding the possibility of self-loops in the graphs.

Bibliography

[1] Matteo Romano, Timoteo Carletti, Anne Lemaitre, and Jérôme Daquin. A network-based risk analysis for space traffic management. *73rd International Astronautical Congress, Paris, France*, 2022.

[2] Matteo Romano, Timoteo Carletti, and Jérôme Daquin. The resident space objects network: a complex system approach for shaping space sustainability. *The Journal of the Astronautical Sciences*, 71(4):31, 2024.

[3] C Pardini and L Anselmo. Impact risk repercussions on the iridium and cosmo-skymed constellations of two recent catastrophic collisions in space, paper id 44. In *4th European Conference for Aero-Space Sciences (EUCASS-2011), Saint Petersburg, Russia*, pages 4–8, 2011.

[4] Astralytical. Global launches: Trends, observations, and opportunities. `https://www.astralytical.com/insights/global-launches-trends-observations-and-opportunities`, 2023.

[5] Donald J Kessler and Burton G Cour-Palais. Collision frequency of artificial satellites: The creation of a debris belt. *Journal of Geophysical Research: Space Physics*, 83 (A6):2637–2646, 1978.

[6] Aerospace America. Understanding the misunderstood kessler syndrome. `https://aerospaceamerica.aiaa.org/features/understanding-the-misunderstood-kessler-syndrome/`, 2024.

[7] Space Impulse. Countries with space programs: An overview. `https://spaceimpulse.com/2023/11/27/countries-with-space-programs-an-overview/`, 2023.

[8] Aerospace Security. Space environment: total launches by country. `https://aerospace.csis.org/data/space-environment-total-launches-by-country/`, 2023.

[9] H ESA. Esa's annual space environment report, gen-db-log-00288-ops-sd, 2023. Fig. 2, page 4/124.

[10] ESA. The current state of space debris. `https://www.esa.int/Space_Safety/Space_Debris/The_current_state_of_space_debris`, 2024.

[11] Inter-Agency Space Debris Coordination Committee et al. Iadc report on the status of the space debris environment. *Issued by IADC Working Group 2/Steering Group*, pages 1–25, 2023.

[12] ESA. Esa commissions world's first space debris removal. `https://www.esa.int/Space_Safety/Clean_Space/ESA_commissions_world_s_first_space_debris_removal`, 2019.

[13] Space Debris User Portal. Space environment statistics. `https://sdup.esoc.esa.int/discosweb/statistics/`, 2022.

[14] ESA. Esa's zero debris approach. `https://www.esa.int/Space_Safety/Clean_Space/ESA_s_Zero_Debris_approach`.

[15] ESA. Clearspace-1. `https://www.esa.int/Space_Safety/ClearSpace-1`, 2020.

[16] L Anselmo and C Pardini. Ranking upper stages in low earth orbit for active removal. *Acta Astronautica*, 122:19–27, 2016.

[17] Joseph N Pelton. A path forward to better space security: Finding new solutions to space debris, space situational awareness and space traffic management. *Journal of Space Safety Engineering*, 6(2):92–100, 2019.

[18] Jericho Locke, Thomas J Colvin, Laura Ratliff, Asaad Abdul-Hamid, and Colin Samples. Cost and benefit analysis of mitigating, tracking, and remediating orbital debris. *Cost and Benefit Analysis of Mitigating, Tracking, and Remediating Orbital Debris*, 2024.

[19] Andy Lawrence, Meredith L Rawls, Moriba Jah, Aaron Boley, Federico Di Vruno, Simon Garrington, Michael Kramer, Samantha Lawler, James Lowenthal, Jonathan McDowell, et al. The case for space environmentalism. *Nature Astronomy*, 6(4): 428–435, 2022.

[20] ESA. About space debris. `https://www.esa.int/Space_Safety/Space_Debris/About_space_debris`, 2022.

[21] Aaron C Boley and Michael Byers. Satellite mega-constellations create risks in low earth orbit, the atmosphere and on earth. *Scientific Reports*, 11(1):1–8, 2021.

[22] Jingrui Zhang, Yifan Cai, Chenbao Xue, Zhirun Xue, and Han Cai. Leo mega constellations: review of development, impact, surveillance, and governance. *Space: Science & Technology*, 2022.

[23] Space.com. Russian anti-satellite missile test was the first of its kind. `https://www.space.com/russia-anti-satellite-missile-test-first-of-its-kind`, 2022.

[24] David Webb. Missile defence—the first steps towards war in space? In *Cyberwar, netwar and the revolution in military affairs*, pages 82–97. Springer, 2006.

[25] Space.com. India's anti-satellite missile test is a big deal. here's why. `https://www.space.com/india-anti-satellite-test-significance.html`, 2022.

[26] Space.com. China's anti-satellite test: Worrisome debris cloud circles earth. `https://www.space.com/3415-china-anti-satellite-test-worrisome-debris-cloud-circles-earth.html`, 2021.

[27] Sebastian Stabroth, Maren Homeister, Michael Oswald, Carsten Wiedemann, Heiner Klinkrad, and Peter Vörsmann. The influence of solid rocket motor retro-burns on the space debris environment. *Advances in Space Research*, 41(7):1054–1062, 2008.

[28] The Aerospace Corporation. A brief history of space debris. `https://aerospace.org/article/brief-history-space-debris`, 2022.

[29] CelesTrak. Norad two-line element set format. `https://celestrak.org/NORAD/documentation/tle-fmt.php`, 2022.

[30] Carmen Pardini and Luciano Anselmo. Revisiting the collision risk with cataloged objects for the iridium and cosmo-skymed satellite constellations. *Acta Astronautica*, 134:23–32, 2017.

[31] Carmen Pardini and Luciano Anselmo. Sdirat: Introducing a new method for orbital debris collision risk assessment. In *Proceedings of the International Symposium on Space Dynamics*, pages 26–30. CNES France, 2000.

[32] Nicholas L Johnson, Paula H Krisko, J-C Liou, and Phillip D Anz-Meador. Nasa's new breakup model of evolve 4.0. *Advances in Space Research*, 28(9):1377–1384, 2001.

[33] Francesca Letizia, Camilla Colombo, Hugh Lewis, and Holger Krag. Extending the ecob space debris index with fragmentation risk estimation. 2017.

[34] Christopher Kebschull, Jonas Radtke, and Holger Krag. Deriving a priority list based on the environmental criticality. *Proc. 65th Int. Astronaut. Congr*, pages 1–9, 2014.

[35] A Rossi, GB Valsecchi, and EM Alessi. The criticality of spacecraft index. *Advances in Space Research*, 56(3):449–460, 2015.

[36] Francesca Letizia, Camilla Colombo, Hugh G Lewis, and Holger Krag. Assessment of breakup severity on operational satellites. *Advances in Space Research*, 58(7): 1255–1274, 2016.

[37] Francesca Letizia, Camilla Colombo, and Hugh G Lewis. Small debris fragments contribution to collision probability for spacecraft in low earth orbits. In *Space Safety is No Accident: The 7th IAASS Conference*, pages 379–387. Springer, 2015.

[38] Juan Luis Gonzalo, Camilla Colombo, and Pierluigi Di Lizia. Analytical framework for space debris collision avoidance maneuver design. *Journal of Guidance, Control, and Dynamics*, 44(3):469–487, 2021.

[39] Christophe Bonnal, Jean-Marc Ruault, and Marie-Christine Desjean. Active debris removal: Recent progress and current trends. *Acta Astronautica*, 85:51–60, 2013.

[40] Jonas Radtke, Sven Mueller, Volker Schaus, and Enrico Stoll. Luca2-an enhanced long-term utility for collision analysis. In *Proceedings of the 7th European Conference on Space Debris*. ESA Space Debris Office Darmstadt, Germany, 2017.

[41] Vitali Braun, André Horstmann, Stijn Lemmens, Carsten Wiedemann, and Lorenz Böttcher. Recent developments in space debris environment modelling, verification and validation with master. In *8th European Conference on Space Debris*, page 18. ESA Space Debris Office Darmstadt, Germany, 2021.

[42] C Martin, C Brandmueller, K Bunte, J Cheese, B Fritsche, H Klinkrad, T Lips, and N Sanchez. A debris risk assessment tool supporting mitigation guidelines. In *4th European Conference on Space Debris*, volume 587, page 345, 2005.

[43] B Bastida Virgili. Delta debris environment long-term analysis. In *Proceedings of the 6th International Conference on Astrodynamics Tools and Techniques (ICATT)*, 2016.

[44] Hugh G Lewis, Graham Swinerd, Neil Williams, and Gavin Gittins. Damage: a dedicated geo debris model framework. In *Space Debris*, volume 473, pages 373–378, 2001.

[45] Deanna L Mains and Marlon E Sorge. The impact satellite fragmentation model. *Acta Astronautica*, 195:547–555, 2022.

[46] J-C Liou. Collision activities in the future orbital debris environment. *Advances in Space Research*, 38(9):2102–2106, 2006.

[47] Mark Matney, Alyssa Manis, Phillip Anz-Meador, Derek Gates, John Seago, Andrew Vavrin, and Y-L Xu. The nasa orbital debris engineering model 3.1: development, verification, and validation. In *International orbital debris conference (IOC)*, number JSC-E-DAA-TN73945, 2019.

[48] DOLADO-PEREZ Jc, D Romain, and REVELIN Bruno. Introducing medee–a new orbital debris evolutionary model. In *Proceeding of the 6th European Conference on Space Debris*, 2013.

[49] Hugh G Lewis, Rebecca J Newland, Graham G Swinerd, and Arrun Saunders. A new analysis of debris mitigation and removal using networks. *Acta Astronautica*, 66 (1-2):257–268, 2010.

[50] Giacomo Acciarini and Massimiliano Vasile. A network-based evolutionary model of the space environment. In *8th European Conference on Space Debris*, pages 1–9, 2021.

[51] Giacomo Acciarini and Massimiliano Vasile. A multi-layer temporal network model of the space environment. In *71st International Astronautical Congress*, 2020.

[52] Emma Stevenson, Victor Rodriguez-Fernandez, Hodei Urrutxua, U Rey, and J Carlos. Towards graph-based machine learning for conjunction assessment. In *Proceedings of the Advanced Maui Optical and Space Surveillance (AMOS) Technologies Conference*, 2022.

[53] D Casanova, C Tardioli, and Anne Lemaitre. Space debris collision avoidance using a three-filter sequence. *Monthly Notices of the Royal Astronomical Society*, 442(4): 3235–3242, 2014.

[54] Petter Holme. *Temporal Networks*, pages 2119–2129. Springer New York, New York, NY, 2014. ISBN 978-1-4614-6170-8. doi: 10.1007/978-1-4614-6170-8_42. URL `https://doi.org/10.1007/978-1-4614-6170-8_42`.

[55] Sudhanshu Chauhan and Nutan Kumar Panda. Chapter 12 - basics of social networks analysis. In Sudhanshu Chauhan and Nutan Kumar Panda, editors, *Hacking Web Intelligence*, pages 217–227. Syngress, Boston, 2015. ISBN 978-0-12-

801867-5. doi: https://doi.org/10.1016/B978-0-12-801867-5.00012-4. URL https://www.sciencedirect.com/science/article/pii/B9780128018675000124.

[56] David Guichard. An introduction to combinatorics and graph theory. *Whitman College-Creative Commons*, 2017.

[57] R. Sahoo, T.S. Rani, and S.D. Bhavani. Chapter 17 - differentiating cancer from normal protein-protein interactions through network analysis. In Quoc Nam Tran and Hamid R. Arabnia, editors, *Emerging Trends in Applications and Infrastructures for Computational Biology, Bioinformatics, and Systems Biology*, Emerging Trends in Computer Science and Applied Computing, pages 253–269. Morgan Kaufmann, Boston, 2016. ISBN 978-0-12-804203-8. doi: https://doi.org/10.1016/B978-0-12-804203-8.00017-1. URL https://www.sciencedirect.com/science/article/pii/B9780128042038000171.

[58] Vito Latora, Vincenzo Nicosia, and Giovanni Russo. *Weighted Networks*, page 374–409. Cambridge University Press, 2017.

[59] David A Vallado and Paul J Cefola. Two-line element sets–practice and use. In *63rd International Astronautical Congress, Naples, Italy*, pages 1–14, 2012.

[60] RED BOOK. Conjunction data message, 2013.

[61] David Vallado and Paul Crawford. Sgp4 orbit determination. In *AIAA/AAS Astrodynamics Specialist Conference and Exhibit*, page 6770, 2008.

[62] Felix R Hoots, Linda L Crawford, and Ronald L Roehrich. An analytic method to determine future close approaches between satellites. *Celestial mechanics*, 33(2): 143–158, 1984.

[63] Petter Holme and Jari Saramäki. A map of approaches to temporal networks. *Temporal network theory*, pages 1–24, 2019.

[64] Todd Andrew Stephenson. An introduction to bayesian network theory and usage. 2000.

[65] Francesca Letizia, Camilla Colombo, and Hugh G Lewis. Collision probability due to space debris clouds through a continuum approach. *Journal of Guidance, Control, and Dynamics*, 39(10):2240–2249, 2016.

[66] Lorenzo Giudici, Mirko Trisolini, and Camilla Colombo. Probabilistic multidimensional debris cloud propagation subject to non-linear dynamics. *Advances in Space Research*, 72(2):129–151, 2023.

[67] TS Kelso et al. Analysis of the iridium 33-cosmos 2251 collision. *Advances in the Astronautical Sciences*, 135(2):1099–1112, 2009.

[68] Megan Ansdell. Active space debris removal: Needs, implications, and recommendations for today's geopolitical environment. *Journal of Public and International Affairs*, 2010.

[69] Noelia Sánchez-Ortiz, Miguel Belló-Mora, and Heiner Klinkrad. Collision avoidance manoeuvres during spacecraft mission lifetime: Risk reduction and required δv. *Advances in Space Research*, 38(9):2107–2116, 2006.

[70] Christophe Bonnal, Darren McKnight, Claude Phipps, Cédric Dupont, Sophie Missonnier, Laurent Lequette, Matthieu Merle, and Simon Rommelaere. Just in time collision avoidance–a review. *Acta Astronautica*, 170:637–651, 2020.

[71] Jonathan C McDowell. The low earth orbit satellite population and impacts of the spacex starlink constellation. *The Astrophysical Journal Letters*, 892(2):L36, 2020.

[72] Taehyun Sung and Jaemyung Ahn. Optimal deployment of satellite mega-constellation. *Acta Astronautica*, 202:653–669, 2023. ISSN 0094-5765. doi: https://doi.org/10.1016/j.actaastro.2022.10.027. URL `https://www.sciencedirect.com/science/article/pii/S0094576522005756`.

[73] Giuseppe Di Pasquale, Brandon Israel Escamilla Estrada, Daniel González-Arribas, Manuel Sanjurjo-Rivo, and Daniel Pérez Grande. Multi-disciplinary optimization of constellation deployment strategies including launcher selection. *Acta Astronautica*, 223:389–403, 2024. ISSN 0094-5765. doi: https://doi.org/10.1016/j.actaastro.2024.07.030. URL `https://www.sciencedirect.com/science/article/pii/S0094576524003989`.

[74] M.E.J. Newman. *Networks: An Introduction*. Oxford University Press, 2010.

[75] Giovanni F Gronchi, Giacomo Tommei, et al. On the uncertainty of the minimal distance between two confocal keplerian orbits. *Discrete and Continuous Dynamical Systems Series B*, 7(4):755, 2007.

A | Appendix A

A further insight in the network theory main concepts is here presented. A network is a group of vertices, or nodes connected by edges, or links. In a graph, vertices have different properties, that are related to how they interact with the other nodes in the network. The coefficient that describe these properties are subsequently stated.
First, there is a need to define a path. In a network, a path is a sequence such that each successive pair of nodes in the path are connected by an edge in the network [74]. A path can be directed when the edges connect all different nodes, and are all directed in the same direction.
The degree centrality, or degree, of a node represents the number of nodes connected to a node i [74]. It can be mathematically formulated as follows (Eq. A.1):

$$D_i = \sum_{j=1}^{n} a_{ij}. \tag{A.1}$$

The betweenness centrality provides, in an unweighted graph, the number of shortest paths that pass through a node i [74]. It describes the importance of a node in connecting different parts of a graph. Its value may be determined through the following Eq. A.2:

$$B_i = \sum_{j=1}^{n} \sum_{k=1}^{n} \sigma_{jk}(i), \tag{A.2}$$

where $\sigma_{jk}(i)$ is the number of shortest paths passing through i.
The closeness centrality represents the mean distance between a node i and all the other nodes in a graph [74]. It can be described as in Eq. A.3:

$$K_i = \frac{1}{n-1} \sum_{\substack{j=1 \\ j \neq i}}^{n} d_{ij}. \tag{A.3}$$

The clustering coefficient is a measure of the density of connections around a specific node.

It can be defined as the number of neighbours of a node i that are connected between each other and the number of pairs of neighbours of i, i.e. the number of triangles created by the connections around i. It can be evaluated as seen in Eq. A.4:

$$C_i = \frac{2}{D_i(D_i - 1)} \sum_{j \neq k}^{n} \sum_{k=1}^{n} a_{ij} a_{ik} a_{jk}. \tag{A.4}$$

B | Appendix B

The three filter sequence exploits three main equations in order to have a way of discerning the nodes that shall pass to the next filter and, ultimately, find a spot in the conjunction list. These equations and ideas have been taken from Casanova, Tardioli, Lemaître research, to which the reader can refer to for further clarification [53].
The first filter is the more straightforward one. It is derived from a method formulated by Hoots et al. [62], where each node is compared to each other object that could collide with it in a perigee-apogee computation. This means that a pair can be discarded if the following Eq. B.1 is satisfied:

$$q - Q \geq D. \tag{B.1}$$

In this equation, q and Q respectively represent the largest perigee and the smallest apogee, while D is a threshold distance. This analysis has been slightly modified, while keeping the same equation in use. The change lays in the use of the maximum and minimum of the function $r_s(t)$, representing the geocentric distance of a RSO s.
The second filter is again a modification of the one proposed by Hoots et al. [62], with ideas taken from Gronchi, Tommei [75]. While Hoots et al. focused on the evaluation of the MOID, comparing it to the threshold distance D, the filter used for the creation of the RSONet revolves around the use of local minimal distances [75]. By comparing the sign of the distances of the couples, it is possible to understand if they undergo an orbit crossing, that would be signaled by a change in sign for one of the two distances [53]. In case a change of sign does not appear, the pair is discarded.
Then, the third filter is a time filter, that compares the cartesian coordinates $X(t)$ and $x(t)$ of the couple with a threshold distance D at any time, according to the Eq. B.2:

$$|X(t) - x(t)| > Datanyt. \tag{B.2}$$

If the inequality here presented is always true, then the couple can be discarded.
The three filter just presented are applied in sequence to all the couples of RSO in the catalogue, in order to derive a conjunction list to be used for the creation of the RSONet.

List of Figures

List of Tables

List of Acronyms

ADR Active Debris Removal i

ARES Assessment of Risk Event Statistics 11

ASAT Anti-Satellite 5

BUM Break-Up Model 9

CAM Collision Avoidance Manoeuvres i

CSI Criticality of Spacecraft Index 10

CDMs Conjunction Data Messages 22

DAMAGE Debris Assessment Mitigation Analysis and Growth Evaluation 11

DELTA Debris Environment Long-Term Analysis 11

DRAMA Debris Risk Assessment and Mitigation Analysis 11

EC Environmental Criticality 10

EOL End-of-Life 3

Acknowledgements

I would like to thank Professor Camilla Colombo for the opportunity offered to work on a thesis related to a field I am incredibly interested in. My thanks go to Prof Jérôme Daquin and Dr. Matteo Romano for their help during the whole period of the thesis and for the opportunity to spend a month in Belgium at the University of Namur. This whole experience has been a truly incredible one, enriching both at academic and personal level. Finally, I want to thank my friends and family for supporting me throughout these years, with special thanks to my parents for all they have done for me.